DOI: 10.1070/RCR4676

Synthetic organometallic models of iron-containing hydrogenases as molecular electrocatalysts for hydrogen evolution or oxidation

Vera V Khrizanforova, Andrey A Karasik, Yulia H Budnikova

A.E.Arbuzov Institute of Organic and Physical Chemistry of Kazan Scientific Centre, Russian Academy of Sciences, Russian Federation
ul. Akademika Arbuzova 8, 420088 Kazan, Russia

Main advances and trends in the development of synthetic analogues of natural iron-containing hydrogenases are analyzed and summarized. The recently synthesized structural and functional analogues of [FeFe]-hydrogenases are described systematically. Some examples of [NiFe]-hydrogenases and the data on their catalytic activity in hydrogen evolution and oxidation reactions in different media, including water, are considered. The extensive potential of this rapidly developing interdisciplinary research area, covering methods of organic and physical chemistry, electrochemistry and biochemistry is showcased. Particular attention is paid to modern approaches to the evaluation of catalytic efficiency of model complexes and to problems of comparing the activities of catalysts.
The bibliography includes 166 references.

Contents

I. Introduction 298
II. Structural and functional analogues of [FeFe]-hydrogenases 301
III. Electrocatalytic hydrogen evolution in acidic aqueous solutions mediated by analogues of [FeFe]-hydrogenases as catalysts 305
IV. Some structural analogues of [NiFe]-hydrogenases 308
V. Functional analogues of [NiFe]-hydrogenases 309
VI. Iron complexes for hydrogen oxidation 311
VII. Assessment of the efficiency of homogeneous electrocatalysts 312
VIII. Conclusion 314

I. Introduction

New efficient and cheap chemical catalysts are urgently needed to meet the requirements of the emerging area of green chemistry. Living organisms produce a plethora of enzymes with high catalytic activity, which can be directly used in biotechnological synthetic systems or be mimicked by researchers. These bioinspired catalysts exploited as nanoreactors hold promise in fuel cell technology and redox processes. Iron is recognized as an essential microelement for bacteria, plants, animals and humans. Although the role of this metal in animal biochemistry is poorly understood, it is iron that is actually responsible for the activity of many bacterial enzymes. Examples are hydrogenases (H_2-ases), methyl-S-coenzyme M methyl reductases (MCRs), peroxidases and nitrogenases, which are efficient catalysts for hydrogen conversion or nitrogen fixation, oxidative transformations and alkylation. In each protein, the environment of Fe has specific features; however, Fe atoms are present in the active sites of all these enzymes and are directly involved in catalytic cycles.

The hydrogen production by electrochemical reduction of a proton donor, ideally water, is an attractive approach to the storage of electrical energy produced by renewable sources, such as solar and wind.[1–3] Although hydrogen evolution reactions (HER) are efficiently catalyzed by platinum group metals in aqueous solutions of acids,[4] it is generally accepted that the high cost and limited natural resources are significant barriers to the use of these metals in large-scale photoelectrochemical or electrochemical production of H_2. In seeking to address this challenge, in the past decade researchers have again focused on the HER catalysis by complexes of transition metals abundant in Earth's crust,[5–8] guided by the idea that their catalytic activity can be controlled by means of targeted ligand

V.V.Khrizanforova. PhD in Chemistry, Junior Researcher at the IOPC KSC RAS.
Telephone: +7(843)279 – 5335, e-mail: khrizanforovavera@yandex.ru
A.A.Karasik. Doctor of Chemical Sciences, Professor, Deputy Director of the same Institute.
Telephone: +7(843)279 – 5335, e-mail: karasik@iopc.ru
Yu.H.Budnikova. Doctor of Chemical Sciences, Head of the Laboratory of the Electrochemical Synthesis at the same Institute,
Telephone: +7(843)279 – 5335, e-mail: yulia@iopc.ru, olefindirector@gmail.com
Current research interests of the authors: physical chemistry, electrochemistry, electrosynthesis, chemistry of heteroorganic compounds, catalysis, nanoparticles, voltammetry, metal complexes, hydrogen power engineering, fuel cells.

Received 24 June 2016
Translation: T.N.Safonova

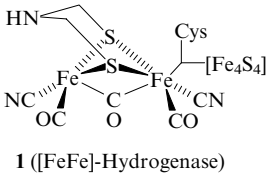
© 2017 Russian Academy of Sciences and Turpion Ltd.

structure design.[9] Despite the problems associated with the use of water as a proton source and as a solvent,[10] latest advances in this area have resulted in the emergence of efficient HER catalysts based on cobalt [11, 12] and nickel.[13]

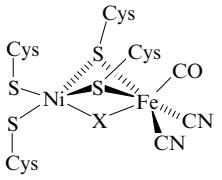
Natural hydrogenases, which are recognized as the most efficient catalysts for the conversion of protons and electrons into hydrogen (and the reverse hydrogen oxidation reaction), have inspired chemists to develop simpler synthetic catalysts, which are structural and functional models of these enzymes, using naturally abundant metals.

Two classes of enzymes incorporating bimetallic active sites that contain iron atoms are [FeFe]-hydrogenases and [NiFe]-hydrogenases,[14, 15] the active sites of which (structures **1** and **2**, respectively) are involved in H_2/H^+ conversions. The third class of hydrogenases, so-called [Fe]-hydrogenases (structure **3**), was found only in methanogens. In these enzymes, H_2 is split at a mononuclear iron-carbonyl centre to release a proton and transfer a hydride ion to the hydride carrier, N^5,N^{10}-methenyltetrahydromethanopterin.[16]

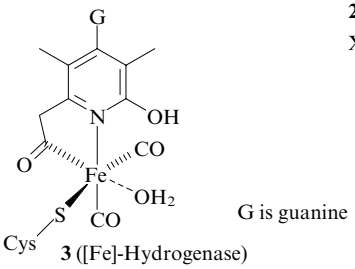
Structures 1 – 3



1 ([FeFe]-Hydrogenase)



2 ([NiFe]-Hydrogenase)
X = O, OH



G is guanine

3 ([Fe]-Hydrogenase)

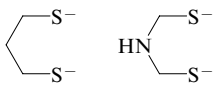
[NiFe]-Hydrogenases are often more active in oxidizing H_2, while [FeFe]-hydrogenases exhibit higher activity in molecular hydrogen production. For example, some [FeFe]-hydrogenases are extremely active in H_2 generation;[17] each enzyme molecule can produce up to $\sim 10^4$ H_2 molecules per second at room temperature.[18] The catalytic activity of [NiFe]-hydrogenases is generally lower.[15] The design of Fe catalysts is of particular interest due to high activity of the natural analogues, the natural abundance of this metal and the lack of environmental toxicity.[19, 20]

The development of HER catalysts based on this metal is essential in order to enhance the economic efficiency of the production of H_2 from water and renewable energy sources.[20] The Fe(TPP) complex (TPP is tetraphenylporphyrin), which catalyzes HER,[21] is one of the first examples. However, the catalytically active iron(0) intermediate, $[(TPP)Fe^0]^{2-}$, is electrochemically generated from $[(TPP)Fe^{III}]^+$ in consecutive steps through three-electron reduction

$$[(TPP)Fe^{III}]^+ \xrightarrow{e^-} [(TPP)Fe^{II}] \xrightarrow{e^-}$$
$$\longrightarrow [(TPP)Fe^{I}]^- \xrightarrow{e^-} [(TPP)Fe^0]^{2-}$$

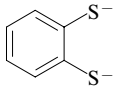
in DMF at a high electrode potential (-1.9 V; unless otherwise stated, all potentials are given with respect to the Fc^+/Fc (ferrocenium cation/ferrocene) reference electrode). Therefore, this complex is of limited practical interest to hydrogen power engineering since the higher the hydrogen evolution potential, the higher the energy cost. Iron complexes with ligands containing electron-withdrawing groups (*e.g.*, pentafluorophenyl) were proposed. For these complexes, the conversion potential to the expected Fe^0 oxidation state is shifted to positive values, and these complexes operate at somewhat more positive potentials than -1.3 V,[22] *i.e.*, the hydrogen evolution becomes easier. Besides, the catalytic activity in H_2 oxidation (the reverse of H^+ reduction) was found for iron complexes with phosphine ligands, in which the pendant amino group of the cyclic ligand functions as a proton relay.[23] Due to a rather flexible spacer, this amino group is located in proximity to the metal centre and, owing to this arrangement, can act as a proton relay, *i.e.*, can transfer hydrogen to the metal and, *vice versa*, binds it as a proton. The presence of this group proved to play a crucial role in the preparation of efficient synthetic hydrogenases. Unfortunately, the sensitivity to oxygen is a major obstacle to the large-scale application of hydrogenases. Nevertheless, the crystallographic characterization of [NiFe]- and [FeFe]-hydrogenases and deeper insight into their functions gained by spectroscopic methods,[15] electrochemistry [24] and theoretical calculations [25] offer new opportunities for the development of synthetic iron-based HER catalysts. The biomimetic approach demonstrated that the active site of [FeFe]-hydrogenases partially resembles the structural features of classical iron thiolate complexes $Fe_2(SR)_2(CO)_6$.[26 – 28] Numerous structural and functional models of [FeFe]-hydrogenases were synthesized and characterized,[29 – 32] in particular, complexes with thiolate ligands **4** – **8** and phosphine ligands **9** – **11**.

Structures 4 – 11

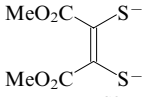


4 (pdt)

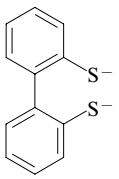
5 (adt^H)



6 (bdt)



7 (dt^{CO_2Me})



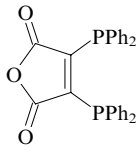
8 (bpdt)



9 (dppe)



10 (dppv)



11 (bma)

Recent advances in this field resulted in the synthesis of iron thiolate complexes possessing characteristic features of the natural enzyme, such as the dithiolate bridge bearing a pendant amino group, the ability to bind terminal hydride, twisted (*i.e.*, with internal strain) geometry and the mixed-valence $Fe^{II}Fe^{I}$ state.[30, 33] It was also found that the catalytic oxidation of H_2 is mediated by a [FeFe]-hydrogenase synthetic model in the oxidized state.[34] Besides, the active artificial enzyme was constructed by incorporating an iron thiolate complex into the protein matrix.[35] This study can be considered as one of the first steps towards the improvement of catalytic activity by means of chemical synthesis and mutagenesis. The structural chemistry of [FeFe]-hydrogenase synthetic models is discussed in several recent reviews.[33, 36 – 39]

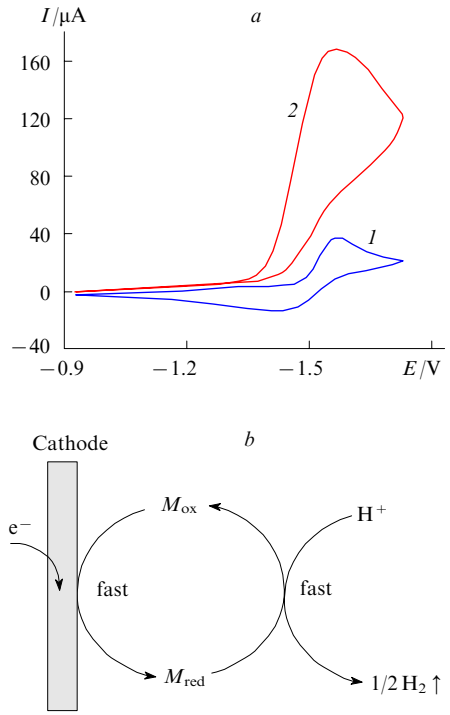


Figure 1. Cyclic voltammograms of a 0.5 mM $Fe_2(bdt)(CO)_5[P(OMe)_3]$ solution in $Bu^n_4NPF_6$–MeCN before (*1*) and after (*2*) the addition of 6 mM TsOH (4-$MeC_6H_4SO_3H$) (*a*)[41] and scheme of the catalytic hydrogen evolution mediated by a Fe complex, where M_{ox} and M_{red} are the starting and catalytically active forms of the complex (*b*).
The catalyst complex is rapidly regenerated at the electrode during the catalytic cycle.

Although water is a preferred proton source for HER, the action of many homogeneous catalysts is studied in acid–organic solvent systems. This choice, which is often dictated by problems of low catalyst solubility and stability, has adverse consequences.

The catalytic characteristics of HER in the presence of transition metal complexes are generally estimated by cyclic voltammetry (CV), in which the catalytically inert electrode, glassy carbon (GC) or mercury, serves as a source of electrons, while the acid that is added to the organic solvent serves as a proton donor. The catalytic activity is estimated from the change observed in the CV response with increasing acid concentration. An increase in the reduction current at a potential close to the reduction potential of the complex (Fig. 1 *a*) or its protonated form is the main criterion.[40,41] If the heterogeneous electron transfer between the electrode and the metal complex and the redox reaction with the substrate (in the case under consideration, with a proton source, such as water, acid and so on) are quite fast (see Fig. 1 *b*), a considerable increase in the catalytic current can be achieved due to a decrease in the electrolysis potential (decrease in the activation energy). Thus, under these conditions, the reduction potential of TsOH at the electrode is −2.0 V; in the presence of a catalyst, −1.5 V. In other words, the catalyst regeneration at the electrode can produce high electrocatalytic current. Therefore, the CV method can be employed to establish the potential at which catalysis occurs and to measure the catalytic current. However, a rigorous analysis of CV responses under varied experimental conditions is required in order to obtain key metrics for the catalytic activity, such as the overpotential and the turnover frequency or number (TOF or TON, respectively),[42] and to determine the mechanism of the catalytic process.[43,44] In its most general definition, the turnover frequency is the amount of the converted substrate (N, moles) per unit time per mole of the catalyst that is contained in the reaction diffusion layer (rather than in the solution bulk). The turnover number characterizes the full activity during the catalyst lifetime (t).

$$\mathrm{TON} = N(\mathrm{substrate})/N(\mathrm{cat.}) = \mathrm{TOF}\cdot t$$

The shift of the potential during the passage of current due to a slow charge transfer step is called the electrochemical polarization or overpotential (η). Methods in organic electrochemistry, terms and electrochemical evaluation of the reactivity of organic and inorganic molecules are covered in more detail in specialized monographs.[45,46]

Apart from electrochemical and related spectroscopic methods,[47,48] computational chemistry methods are increasingly used both to analyze experimental data and to determine the mechanisms of catalysis.[49] The density functional theory has proved particularly useful for the determination of the structures of intermediates and transition states of the catalytic system and for the estimation of their physicochemical properties, such the acidity constant and the standard electrochemical potential.[50,51] In recent years, computational methods have been applied in combination with kinetic analysis to calculate TOF of catalysts in electrochemical reactions.[52–54]

It should be noted that although recent investigations provided extensive data on the structures and mechanisms of action of [FeFe]-hydrogenases, unfortunately only some structural analogues proved to be efficient, *i.e.*, the number of functional analogues acting as efficient electrocatalysts for H_2 production is much smaller. Although the absolute majority of researchers channeled their efforts to modelling the active site of natural [FeFe]-hydrogenases, it cannot be ruled out that new structures will be developed, in which the active site of the complex will be noticeably or totally different from the environment of the iron atom in the enzyme. In other words, one cannot exclude the possibility that other iron complexes, the structures of which differ from or only partially resemble natural enzymes, will display better electrocatalytic properties. For example, there is a large number of iron complexes containing classical ligands, such as cyclopentadienyl (η^5-C_5H_5, Cp), bridging and(or) terminal CO and bridging ligands (*e.g.*, alkyl, alkynyl, alkenyl, allyl, allenyl and so on), some redox-active ligands and clathrochelates, which can be considered as potential electrocatalysts for H_2 evolution.[55–57] New ligands possessing different donor–acceptor properties, steric and other characteristics may play a crucial role in investigations of the catalytic activity of model systems. Researchers focus their efforts on designing such synthetic analogues of hydrogenases, which would function at room temperature in aqueous or weakly acidic media at nearly zero or low overpotentials for hydrogen evolution but with comparable or even higher values of TOF and TON.

This review considers recent advances in the synthesis of structural and functional analogues of iron-containing hydrogenases with emphasis on functional analogues serving as models; selected examples of [NiFe]-hydrogenase

analogues are given; approaches to the most rational comparative analysis of the catalytic activity of homogeneous catalysts for electrochemical hydrogen evolution are discussed considering characteristics available in the literature.

II. Structural and functional analogues of [FeFe]-hydrogenases

As mentioned above, the hydrogen production through proton reduction, as well as hydrogen oxidation, are naturally catalyzed by the enzymes hydrogenases. Two genetically distinct hydrogenases were identified. These enzymes were found to contain fragments of Ni and(or) Fe thiolate complexes with CN and CO ligands. Generally, these enzymes are Fe – S cluster rich, which is indicative of the central role of electron transfer involving Fe atoms.[14, 58] [FeFe]-Hydrogenases are more active than [NiFe]-hydrogenases and they most often function as catalysts for H_2 production (Table 1).[14, 15, 17, 18]

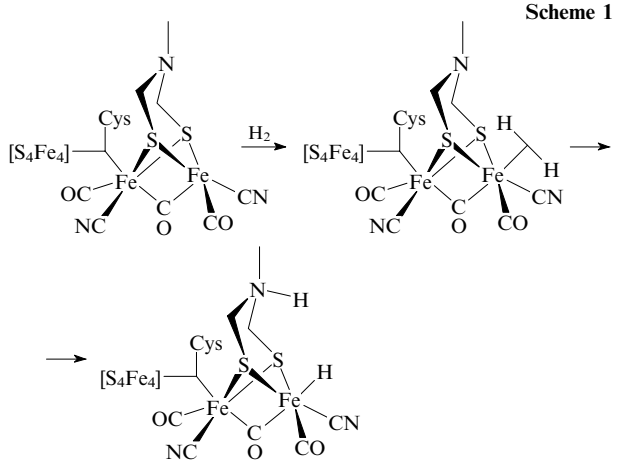
Table 1. Activity of [FeFe]- and [NiFe]-hydrogenases.[14, 15, 59]

Reaction	Reaction rate [a]	
	[FeFe]-hydrogenase	[NiFe]-hydrogenase
H_2 oxidation	28 000	700
H_2 production	6000 – 9000	700

[a] The rates are given in moles of H_2 per mole of the enzyme per second and were measured at 30 °C.

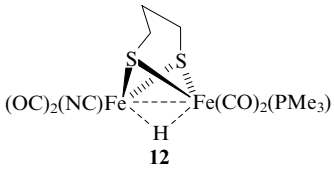
In [FeFe]-hydrogenases, one Fe_4S_4 cluster is directly linked to the active site containing two Fe atoms. The 6Fe ensemble is called the H-cluster. Scheme 1 displays the simplified structure of the [FeFe]-hydrogenase active site and presents its reaction with hydrogen. This scheme shows only the enzyme active site and does not present the structure of the remainder of the protein molecule. The electron transfer occurs through the Fe_4S_4 cluster and the proton (hydrogen) is delivered to the desired active site through channels (not shown in Scheme 1), which ensures the precise reagent delivery and release of the products from the catalytically active metal centre. The putative mechanism of H_2 oxidation involves the binding of H_2 to the Fe centre followed by the heterolytic cleavage of the hydrogen molecule to form iron hydride and the proton migration to the nitrogen atom.[60] Several research groups succeeded in synthesizing and characterizing the structural analogues of [FeFe]-hydrogenases, which catalyze processes similar to the reactions catalyzed by natural enzymes.[31, 61 – 65]

Scheme 1

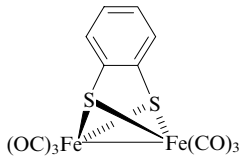


Rauchfuss and co-workers[40, 63, 66] found that hydride-bridged dinuclear iron complex **12** catalyzes the hydrogen production from *p*-toluenesulfonic acid. The catalytic reaction proceeds at a potential of −1.43 V with an overpotential of 0.78 V.

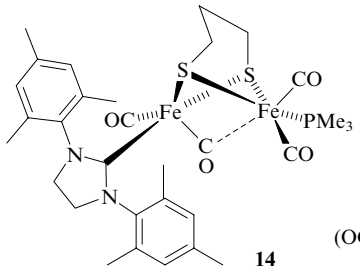
Structures 12 – 16



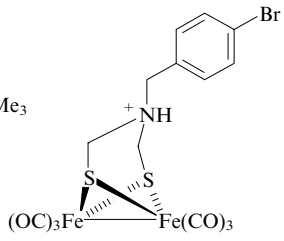
12



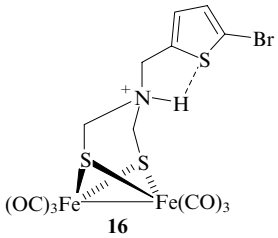
13



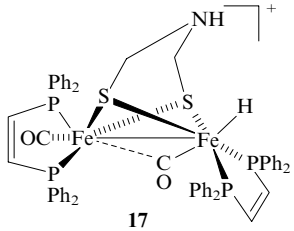
14



15



16



17

Darensbourg and co-workers[67] successfully used the complex $[Fe_2(CO)_5(PTA)\{\mu\text{-}S(CH_2)_3S\}]$ (PTA is 1,3,5-triaza-7-phosphaadamantane) for hydrogen generation from acetic acid at a potential of −1.4 V in a MeCN – H_2O mixture. Gloaguen[41] employed neutral hydride Fe_2S_2 complex **13** for electrocatalytic reduction of HOTs; in this process, the protonation is preceded by the reduction of complex **13** to the dianionic form. Lichtenberger and co-workers[68] also reported the hydrogen evolution from acetic acid catalyzed by complex **13** at a potential of −2.1 V. Liu and Darensbourg[69] synthesized complex **14** with the N-heterocyclic carbene ligand at one of Fe centres. This paramagnetic $Fe^{I}Fe^{II}$ complex bears a semi-bridging carbonyl ligand and has the open coordination site similar to the active Fe – Fe fragment in [FeFe]-hydrogenase.

Several research teams succeeded in synthesizing dinuclear Fe complexes with dithiolate ligands structurally similar to those shown in Scheme 1. Ott and co-workers[70] prepared a Fe_2S_2 complex with the dithiolate ligand and the intraligand base (nitrogen atom), which is protonated by perchloric acid to form complex **15**. The reduction of protonated complex **15** is 400 mV earlier than the reduction of the starting complex: in the presence of excess perchloric acid, the hydrogen evolution is observed at a potential of −1.48 V.[70] Sun and co-workers[71] synthesized Fe_2S_2 complex **16** containing the thiophene moiety in the dithiolate ligand. The protonated form of complex **16** catalyzes the

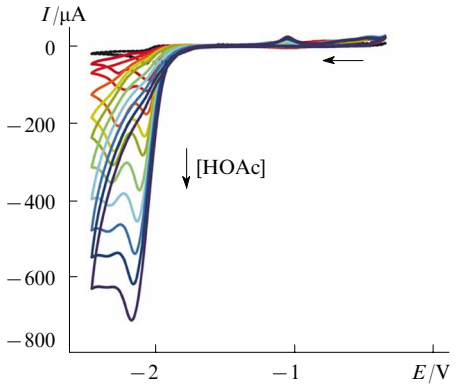


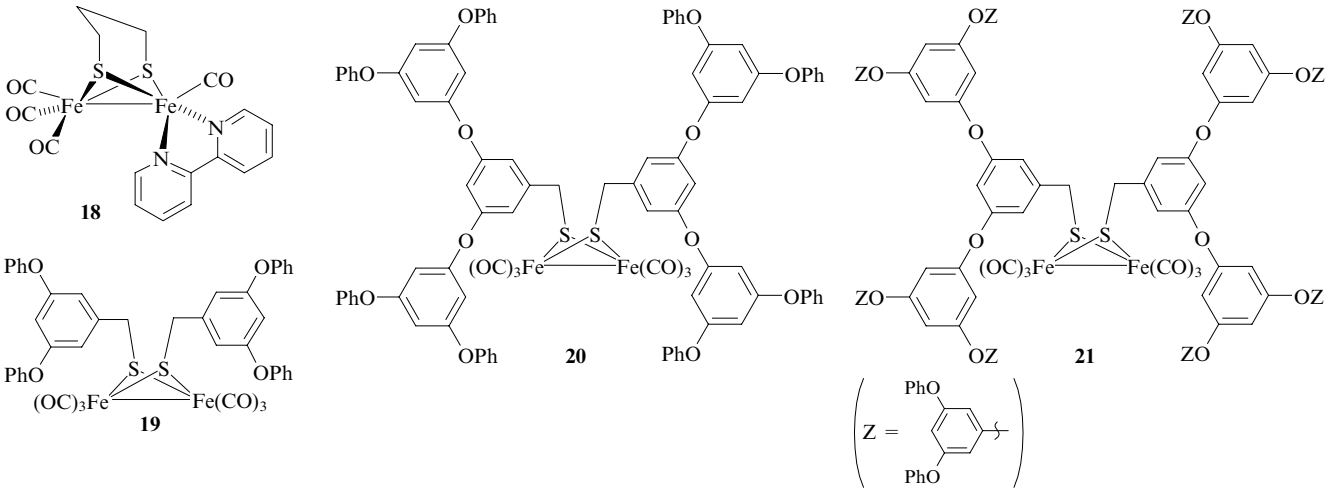
Figure 2. Cyclic voltammograms of Roy's complex **18**.[73] The concentration of complex **18** is 1.4 mmol litre^{-1}, the concentration of acetic acid ranges from 0 to 42 mmol litre^{-1} in MeCN.

reduction of perchloric acid at a potential of −1.09 V, which proved to be the best value compared to other $Fe_2(CO)_6$ complexes. Rauchfuss and co-workers[72] found that complex **17** catalyzes the reduction of strong acids at −20 °C to produce H_2 at −1.5 V; the low temperature was used to diminish isomerization accompanied by the transformation of the terminal hydride into the bridging one.[72] Therefore, these data demonstrate that the above-described Fe_2S_2 complexes function only in strongly acidic media at rather high cathodic potentials, *i.e.*, their efficiency is not comparable to that of the natural enzymes.

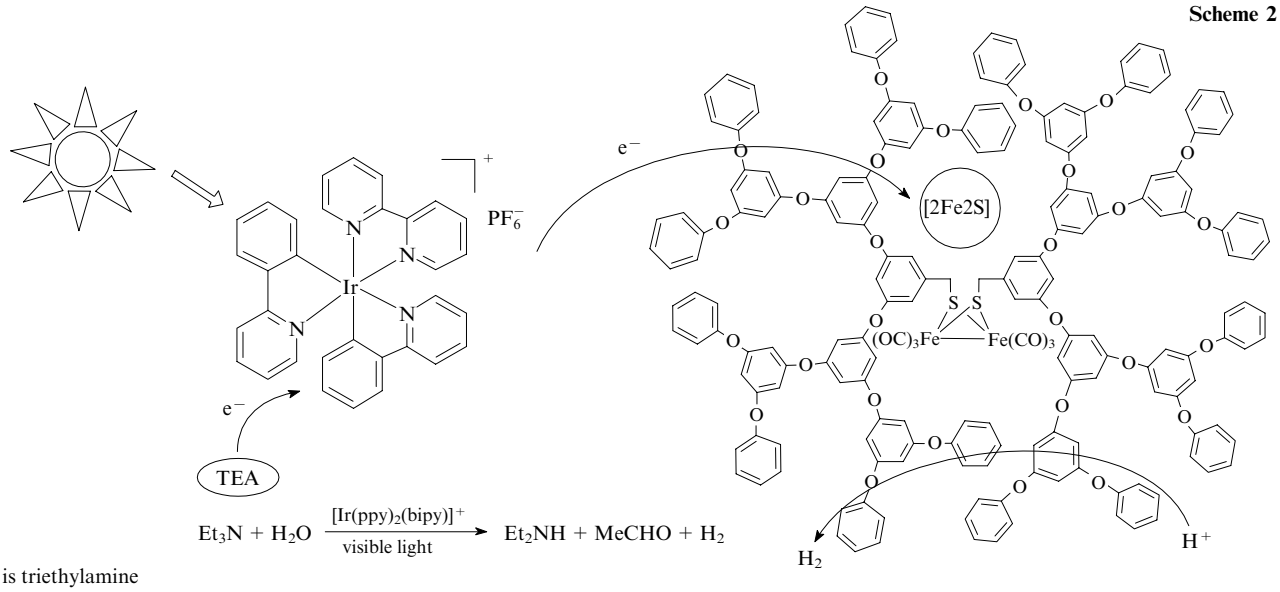
The research team headed by Roy[73] synthesized new complex **18** containing the Fe_2S_2 fragment stabilized by the bipyridine ligand. In the presence of acetic acid, this complex exhibits a 12-fold current enhancement at a very high negative potential (−2.06 V) (Fig. 2). In the presence of stronger acids (HBF_4, TsOH), the catalytic process starts at a potential of −1.3 to −1.4 V, which is 0.7–0.8 V lower than that in the case of acetic acid, *i.e.*, this process is energetically more favourable.[73]

Relying on the crystal structure analysis of fragments of [NiFe]-hydrogenases, it was concluded that the active site of the enzyme is shielded by a protein shell, thus providing its protection without decreasing the catalytic activity. Taking into account these structural features of natural hydro-

Structures 18 – 21

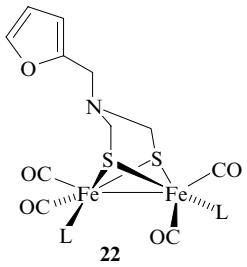


Scheme 2

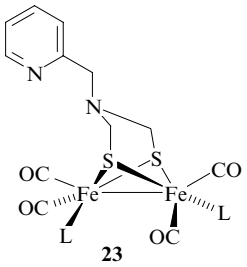


TEA is triethylamine

Structures 22 – 25

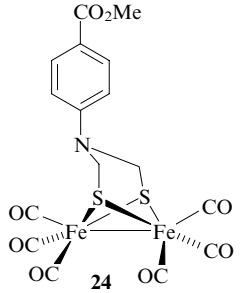


22

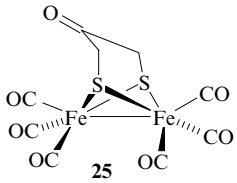


23

L is 1,3-dimethylimidazol-2-ylidene



24



25

genases, Li's research team [74] synthesized dendrimer complexes **19** – **21**, which proved to be efficient catalysts for photochemical hydrogen evolution. The homogeneous three-component catalytic system was composed of an Ir^{III} complex as the photosensitizer, synthetic hydrogenase (**19** – **21**) as the proton reduction catalyst and triethylamine as the sacrificial electron donor (Scheme 2). The turnover frequency of the catalytic cycle for these complexes was 6190 – 7240 h^{-1}, and the quantum yield of photocatalytic hydrogen evolution was up to 28%. It was hypothesized that the catalytic process is intermolecular and involves the protonation of the $Fe^{I}Fe^{I}$ centre to form the $HFe^{II}Fe^{I}$ fragment and the subsequent reduction and protonation of the latter fragment, resulting in hydrogen evolution and regeneration of the $Fe^{I}Fe^{I}$ centre.[74]

In the first example of the electrochemical H_2 evolution catalyzed by a biomimetic iron dithiolate complex,[66] a strong acid (H_2SO_4) was used. In this process, the catalyst exhibited low efficiency (turnover number of H_2 evolution was 6 with an overpotential of 0.82 V at −1.40 V in MeCN). Strong acids [H_2SO_4, HBF_4, $HClO_4$, HCl, CF_3SO_3H (TfOH)] are usually unsuitable for synthetic

Table 2. Electrocatalytic hydrogen evolution in the presence of complexes **22** – **25**.[58, 59, 75]

Complex	Catalytic peak potential /E_p	Overpotential /V	Catalytic efficiency [a]
22	−1.51	0.62	0.29
23	−1.72	0.83	0.60
24	−1.60	0.71	0.34
25	−1.48	0.59	0.33

Note. CF_3CO_2H was used as the proton source [$pK_a^{MeCN} = 12.7$, $E^{MeCN}(HA/H_2) = -0.89$ V].

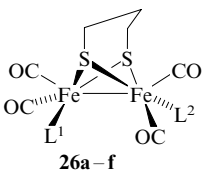
[a] Determined as $(i_{cat}/i_d)/(c_{HA}/c_{cat})$, where i_{cat} is the catalytic current, i_d is the reduction current for the catalyst in the absence of an acid, c_{HA} and c_{cat} are the acid and catalyst concentrations, respectively.

analogues of [FeFe]-hydrogenases because of high overpotentials for hydrogen evolution (> 0.7 – 2.0 V) and instability in a strongly acidic medium.[13] Only a few examples of the H_2 production using medium-strength acids ($pK_a = 10 - 15$) were described; the moderate efficiency and overpotentials in the range of 0.4 – 1.2 V in MeCN were obtained.[58, 59, 75] The results of electrocatalytic proton reduction from CF_3CO_2H in the presence of Fe_2S_2 complexes **22** – **25** are summarized in Table 2.

Weak acids ($pK_a > 15$, $ClCH_2CO_2H$, $NCCH_2CO_2H$, Et_3NH^+, AcOH and $PhCO_2H$) were commonly used as proton sources in electrocatalytic reactions mediated by Fe_2S_2 complexes. In the presence of these weak acids in MeCN, the overpotential varies from −0.2 to −1.0 V.[31]

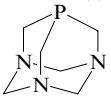
More than 70 examples of the electrocatalytic H_2 evolution mediated by dinuclear iron complexes in the presence of weak acids were reported. However, the data on the relationship between the structure and electrocatalytic efficiency of [FeFe]-hydrogenase analogues are scarce, because the results were obtained using different electrodes, acids, catalyst concentrations and different solvents. Therefore, the published data are difficult to compare. A comparison of the catalytic results, for example, for HOAc in MeCN, provides an insight into the influence of the ligands on the electrocatalytic properties of complexes in the proton reduction. The electrocatalytic parameters for complexes **26** – **33** are given in Tables 3 and 4.[67, 76 – 85]

Structures 26 – 33

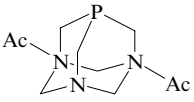


26a – f

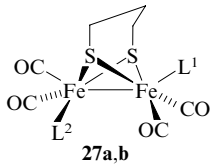
$L^1 = L^2 = CO$ (**a**), PTA (**c**), PMe_3 (**d**), DAPTA (**f**); $L^1 = CO$: L^2 = PTA (**b**), DAPTA (**e**)



PTA

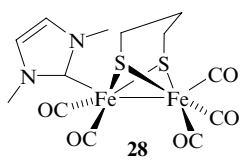


DAPTA

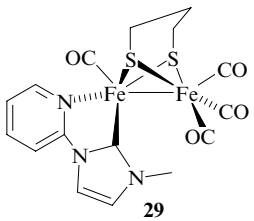


27a,b

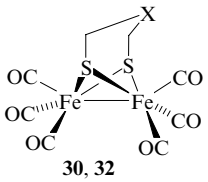
$L^1 = PPh_2$(2-pic): $L^2 = CO$ (**a**), PMe_3 (**b**) (pic is 2-picolyl)



28

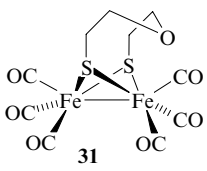


29

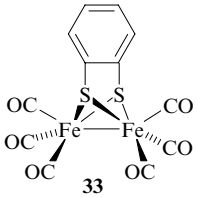


30, **32**

X = O (**30**), NC_6H_4OMe-4 (**32**)



31



33

Table 3. Influence of the nature and arrangement of the ligands on the electrocatalytic properties of dinuclear iron complexes **26**–**29** [$E^{MeCN}(AcOH/H_2) = -1.46$ V].[67, 76–78]

Complex	E_p/V	Overpotential/V	Catalytic efficiency	Concentration of HOAc/mmol litre^{-1}	Concentration of complex/mmol litre^{-1}
26a	−2.35	0.89	0.06	100	2.0
26b	−1.94	0.48	0.03	100	2.0
26c	−2.18	0.72	0.08	100	2.0
26d	−2.25	0.79	0.11	100	2.0
26e	−1.83	0.37	0.43	4	1.0
26f	−2.00	0.54	0.65	4	1.0
27a	−1.86	0.40	0.43	5	1.0
27b	−2.20	0.74	0.70	5	1.0
28	−2.08	0.62	0.19	10	1.0
29	−2.16	0.70	1.10	10	1.0

Table 4. Influence of the nature of the dithiolate moiety on the electrocatalytic properties of dinuclear iron complexes **30**–**33** [$E^{MeCN}(AcOH/H_2) = -1.46$ V].[79–82]

Complex	E_p/V	Overpotential/V	Catalytic efficiency	Concentration of HOAc/mmol litre^{-1}
30	−2.20	0.74	0.40	10
31	−2.28	0.82	0.91	10
32	−2.10	0.64	0.19	10
33	−2.11	0.65	0.64	5

Complexes **26**–**32** are reduced in two one-electron steps, which are assigned to Fe^IFe^I/Fe^IFe^0 and Fe^IFe^0/Fe^0Fe^0 redox transitions. In the case of Fe_2S_2 complexes containing only CO ligands, the electrocatalytic proton reduction in the presence of acetic acid usually occurs at the second peak potential, at which a catalytic current is observed at high overpotentials, rather than at the first peak potential. The electrocatalytic activity in H_2 generation reactions at the first reduction peak potentials is observed upon the replacement of one or two CO ligands with PR_3, N-heterocyclic carbene or another ligand. Therefore, the introduction of a strong electron-donor ligand into Fe_2S_2 complexes leads to an apparent decrease in both the overpotential and efficiency (*cf.* complexes **26a**,**b** in Table 3).[67]

A comparison of the data for pairs of complexes **26b**,**c**, **26e**,**f**,[76] **27a**,**b** (see Ref. 77) demonstrates that the replacement of the second CO ligand leads to a considerable increase in the overpotential and catalytic efficiency (see Table 3). Complexes of Fe_2S_2 with strong electron-donor ligands exhibit high overpotentials and higher efficiency compared to the complexes with weak electron-donor ligands (*cf.* **26c** and **26d**, **26f** and **27b**). Data for complexes **28** and **29** show that the introduction of a chelating ligand giving an unsymmetrically disubstituted Fe_2S_2 complex leads to a considerable enhancement of the efficiency and an increase in the overpotential to 0.7 V.[78]

Another way of tuning the electronic properties of [FeFe]-hydrogenase analogues is based on a change in the nature of the dithiolate group. Table 4 summarizes data on the electrocatalytic properties of four model Fe_2S_2 complexes containing only CO ligands, which were obtained under similar conditions. It should be noted that the catalytic efficiency of SCH_2OCH_2S-bridged complex **30** is lower than that of complex **31** containing a more flexible bridge ($SCH_2CH_2OCH_2CH_2S$), while the overpotential increases only slightly (0.74 and 0.82 V for complexes **30** and **31**, respectively).[79, 80]

The replacement of the $S(CH_2)_3S$ bridge (complex **26a**) by the SCH_2OCH_2S (complex **30**),[79] $S(CH_2)_2O(CH_2)_2S$ (**31**)[80] or SCH_2NRCH_2S (**32**) group[81] provides another example of the enhancement of the efficiency accompanied by a decrease in the overpotential for proton reduction. Complexes **30**–**32** bearing oxygen or nitrogen atoms at the midpoint of the bridge exhibit higher efficiency at lower overpotentials compared to complex **26a**, which can be attributed to the presence of the internal basic centre.

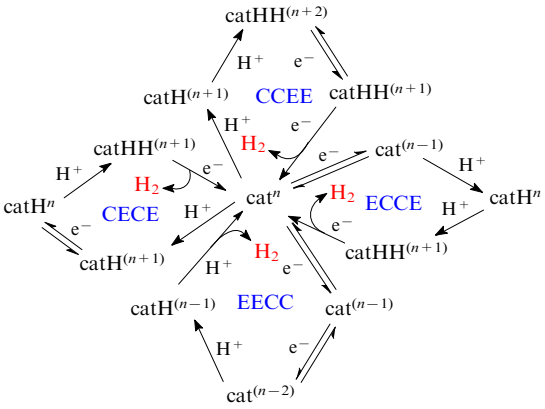
Complex **33** having a rigid conjugated bridge displays radically different electrochemical properties compared to most of Fe_2S_2 complexes with flexible bridges. For example, the electrochemically reversible two-electron reduction of complex **33** in MeCN gives the dianion at a potential of −1.27 V,[82, 83] while complex **26a** has the first one-electron reduction peak at −1.65 V and the second irreversible peak at a potential of −2.25 V.[76] Reduced forms of Fe_2S_2 complexes containing aromatic moieties in the bridge are strongly stabilized by the benzene ring. Therefore, complex **33** is a more efficient and stable catalyst for electrochemical proton reduction than other Fe_2S_2 analogues.[84, 85] The catalysis occurs at a potential, at which complex **33** is not electroactive. In the presence of weak acids, the overpotential for hydrogen evolution ranges from 0.44 to 0.77 V, and the efficiency varies from moderate to high. For example, the catalytic efficiency with the use of chloroacetic acid as a proton donor is 0.96 at an overpotential of 0.77 V. This corresponds to efficient catalysis, in which the current is limited by the diffusion of acid to the electrode.

Taking into account such advantages of complex **33** as a lower reduction potential compared to other Fe_2S_2 complexes, the simultaneous transfer of two electrons and good stability of the reduced form of the catalyst, this class of catalysts is worthy of further in-depth investigation in order to use these complexes for both the electro- and photocatalytic H_2 production.

Mechanisms of electrochemical production of H_2 catalyzed by Fe_2S_2 complexes depend on the basicity of Fe_2 centres, internal bases and ligands in the catalysts, as well as on the reaction conditions (the nature of the acid used, the medium and so on). Four possible pathways of the electrocatalytic generation of H_2 mediated by Fe_2S_2 complexes were described. These pathways are denoted as EECC, ECCE, CECE and CCEE (Scheme 3) (in electochemistry,

the reaction mechanisms are represented by a sequence of letters referred to the names of individual steps in the general scheme, where E is an electrochemical step and C is a chemical one). The EECC mechanism was proposed for the electrochemical H_2 evolution in the presence of a weak acid (HOAc) in MeCN catalyzed by Fe_2S_2 complexes containing only CO ligands, while the ECCE mechanism is realized for PR_3-substituted complexes.[67] The CECE pathway is likely for PR_3-substituted Fe_2S_2 complexes, which do not contain the internal basic centre in the ligand structure, when a stronger acid (TsOH) is used as the proton source and the protonation occurs at the metal centre.[86] The CECE mechanism is also possible for catalysts containing an internal base that acts as a proton relay; generally, an amine nitrogen atom serves as the internal base if pK_a of the acid used corresponds to its basicity.[87] In the presence of a strong base (H_2SO_4) in MeCN, the H_2 evolution catalyzed by $[(\mu\text{-pdt})\{Fe(CO)_2(PMe_3)\}\{Fe(CO)_2(CN)\}]^-$ apparently proceeds *via* the CCEE mechanism.[56] Besides, the ECEC mechanism was proposed for photochemical H_2 evolution,[88] but it is not typical of electrochemical catalytic reactions mediated by Fe_2S_2 complexes.

Scheme 3



cat is the catalyst; $n = 0, -1, -2$

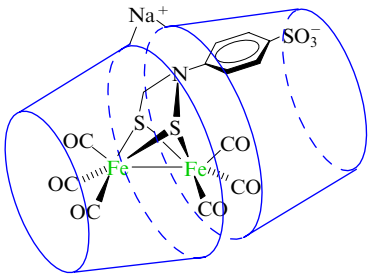
III. Electrocatalytic hydrogen evolution in acidic aqueous solutions mediated by analogues of [FeFe]-hydrogenases as catalysts

Water solubility, at least to a certain extent, is a desirable property for catalysts enployed for H_2 evolution because the ultimate aim is to design a catalyst suitable for both the proton reduction and water oxidation. Most of iron-based molecular catalysts are soluble only in organic solvents. Therefore, investigations of the electrocatalytic production of H_2 using these catalysts are usually performed in organic solvents, such as MeCN, DMF or THF, in the presence of different acids. Some attempts were made to increase water solubility of Fe_2S_2 complexes by introducing hydrophylic phosphine ligands, such as PTA,[76] DAPTA (3,7-diacetyl-1,3,7-triaza-5-phosphabicyclo[3.3.1]nonane),[77,89] $P(CH_2OH)_3$ (Ref. 90) and $P(CH_2CH_2CO_2H)_3$.[91] The complexes $[(\mu\text{-pdt})\{Fe(CO)_3\}\{Fe(CO)_2PTA\}]$ (**26b**) and $[(\mu\text{-pdt})\{Fe(CO)_2PTA\}_2]$ (**26c**) are readily soluble in the MeCN – H_2O mixture (1 : 1) and can catalyze proton reduction from HOAc in this medium with overpotentials of 0.48 and 0.72 V, respectively.

Complexes of Fe_2S_2 with a DAPTA ligand are much better soluble in water than their PMe_3 and PTA analogues. Researcher Consequently, the complexes $[(\mu\text{-pdt})\{Fe(CO)_2PTA\}\{Fe(CO)_2DAPTA\}]$ (**26e**) and $[(\mu\text{-pdt})\{Fe(CO)_2DAPTA\}_2]$ (**26f**) can be used for the electrochemical reduction of protons from HOAc in water at −1.3 V with respect to SHE (standard hydrogen electrode).

Darensbourg and co-workers[92] characterized supramolecular host – guest complex **34**, in which the Fe_2S_2 complex is incorporated into the β-cyclodextrin cavity (β-CD, represented as a truncated cone), to mimic the protein environment of [FeFe]-hydrogenases.

Structure 34



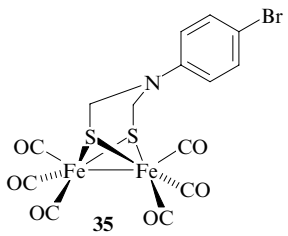
34

Dinuclear Fe inclusion complex **34** is readily soluble in water, and its cyclic voltammogram shows a small catalytic peak at −1.4 V *versus* Ag/AgCl in the presence of acetic acid in an aqueous NaCl solution. Despite the fast exchange of the Fe_2S_2 complex in an aqueous solution, this host – guest system is the first example that mimics the protein environment for a small molecular model of the [FeFe]-hydrogenase active site.

Known examples of H_2 generation catalyzed by Fe_2S_2 complexes in water exhibit rather low efficiency at overpotentials > 0.9 V. The use of water as the only source of protons (in the absence of acids) is still a long-term challenge, which can be solved by studying the principal characteristics of natural hydrogenases and their activity in H_2 evolution and oxidation reactions.

Dey *et al.*[93] investigated the electrochemical hydrogen production in acidified water using model azadithiolate-bridged complex **35** and studied the role of solvation in an aqueous solution in the lowering of the overpotential. It was demonstrated that complex **35** is an efficient catalyst for hydrogen evolution from an aqueous H_2SO_4 solution (pH < 3) with a turnover number up to 6400 s^{-1} at −0.5 V; the current efficiency is >95%. The authors succeeded in immobilizing the complex on a carbon cathode, which is of practical interest. This is the first report about the heterogeneous electrochemical production of hydrogen in an acidic aqueous medium mediated by the Fe_2S_2 complex with the bridging azadithiolate ligand.

Structure 35



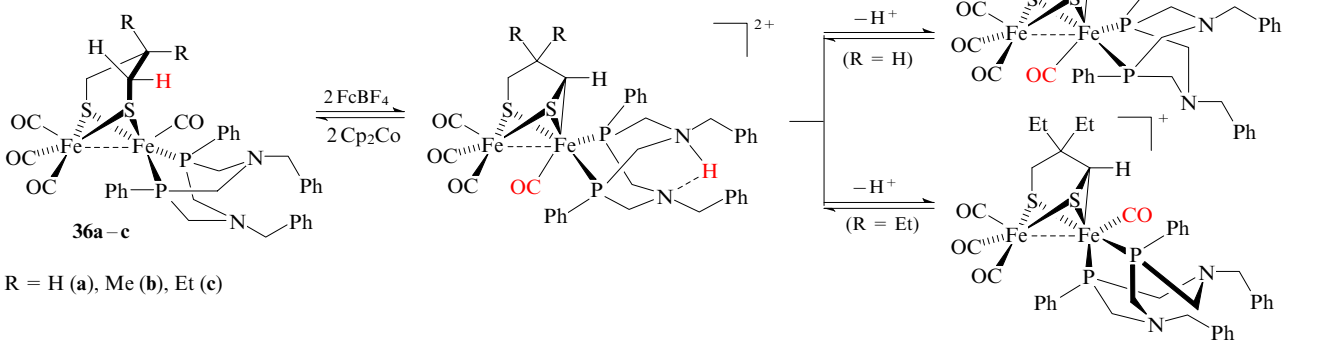
35

Recently, Zheng *et al.*[94] synthesized a series of pendant-amine-containing Fe_2S_2 complexes **36a – c** $[R_2C(CH_2S\text{-}\mu)_2\{Fe(CO)_3\}\{Fe(CO)(P_2^{Ph}N_2^{Bn})\}]$ [R = H (**a**), Me (**b**), Et (**c**); $P_2^{Ph}N_2^{Bn}$ is 1,5-dibenzyl-3,7-diphenyl-1,5-diaza-3,7-diphosphacyclooctane] with different substituents at the bridgehead carbon atom of the thiolate linker. These complexes can undergo reversible intramolecular $C(sp^3)-H$ heterolysis (Scheme 4). Two-electron oxidation and reduction reactions afford $Fe^{II}Fe^{II}$ complexes with different configurations regardless of the bulkiness of the substituent at the bridgehead position. In the presence of HBF_4, these reactions do not lead to catalytic hydrogen evolution.

Voloshin's research team[57,95] proposed using iron and cobalt hexabromoclathrochelates **37a**,**b** and **38** as hydrogen evolution catalysts. The addition of $HClO_4$ to a solution of these clathrochelates in acetonitrile gave rise to catalytic waves at a potential of the Fe^{2+}/Fe^{+} redox couple. A much smaller increase in the catalytic current (I_{cat}) was observed for clathrochelate **37a** as compared with its cobalt-containing analogue **37b**. Controlled-potential electrolysis also confirmed higher activity of the Co derivative. Thus, the faradic yield of H_2 for this cobalt complex is 35% *versus* ~19% for the Fe complex. Rather low yields can be attributed either to relatively high overpotentials or low chemical stability of these complexes in the presence of perchloric acid.

Carroll and co-workers[96] performed a comparative study of biomimetic hydrogen evolution catalysts, which either contain or do not contain an amine cofactor in the ligand (adt^H): $Fe_2(adt^H)(CO)_2(dppv)_2$ (**39**) and $Fe_2(pdt)(CO)_2(dppv)_2$ (**40**) (adt^H = **5**, pdt = **4**, dppv = **10**). These compounds are structurally and stereodynamically very similar, have similar NMR spectra but exhibit strongly different catalytic properties. The protonation of complexes **39** and **40** gives three isomeric Fe hydrides, beginning with the kinetically favoured terminal hydride (t-H), which is sequentially converted into symmetrical and unsymmetrical isomers of bridging hydrides (Scheme 5). For complex **39**, the corresponding Fe hydrides protonated at the NH group were also observed. In the case of terminal [t-H-**39**]BF_4, the equilibrium of protonation is sensitive to counterions and the solvent. The compound [t-H-$\mathbf{39}^H$]$(BF_4)_2$ represents the first example of crystallographically characterized terminal Fe hydrides[96] produced by the protonation. The NH···HFe distance equal to 1.88(7) Å attests to dihydrogen bonding (the sum of the van der Waals radii of two H atoms is 2.4 Å). The bridging hydrides [μ-H-**39**]$^+$ and [μ-H-**40**]$^+$ are reduced at about −1.8 V, *i.e.*, at 150 mV more negative potentials than the terminal hydrides [t-H-**39**]$^+$ and [t-H-**40**]$^+$ (at −1.65 V). The reduction of the amine structures of the Fe hydrides [t-H-**39**]$^+$ and [t-H-$\mathbf{39}^H$]$^{2+}$ is irreversible. For pdt analogue **40**, the reduction current peak of [t-H-**40**]$^{+/0}$ in the cyclic voltammogram is independent of additives of weak acids [pK_a (MeCN) = 15.3], but a catalytic growth of this peak is observed in the presence of $HBF_4 \cdot Et_2O$, although the turnover frequency is small (~4 s^{-1}), while the overpotential for hydrogen evolution is high (> 1 V). The cyclic voltammogram of [t-H-**39**]$^+$ strongly depends on the relative acid strength, and the catalyst regeneration occurs with TOF = 5000 s^{-1} at an overpotential of 0.7 V.[96] The protonated Fe hydride complex [t-H-$\mathbf{39}^H$]$^{2+}$ is a more efficient catalyst. Thus, the TOF for this complex was estimated at 58 000 s^{-1} with an over-

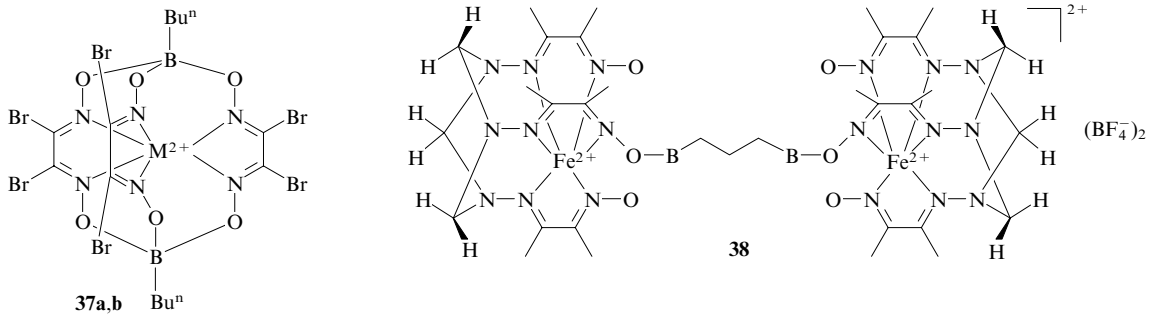
Scheme 4



36a – c

R = H (**a**), Me (**b**), Et (**c**)

Structures 37, 38

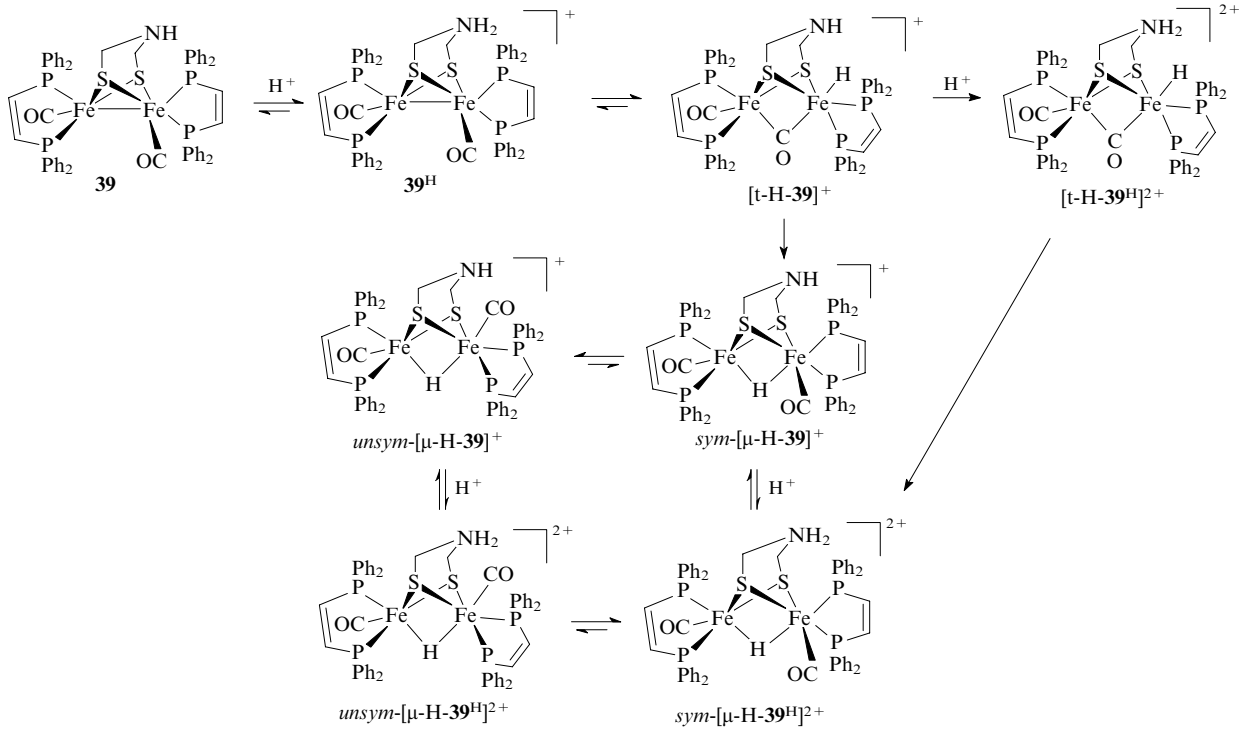


37a,**b**

M = Fe (**a**), Co (**b**)

38

Scheme 5



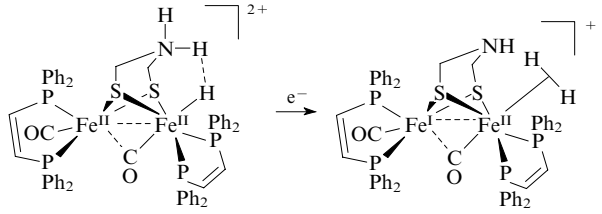
potential of 0.5 V. This is the highest currently known value of TOF for synthetic Fe-hydrogenases.[96]

The hydrogen evolution in the presence of biomimetic iron dithiolates is accelerated by the amine cofactor located in proximity to the hydride ligand. Protonated derivatives **39** and **40** have quite different catalytic properties although the neutral complexes are spectroscopically almost indistinguishable. Therefore, the adt^{H} and pdt ligands have comparable inductive effects with the result that the complexes display very similar thermodynamic properties.

The crystallographic analysis of [t-H-**39**^{H}]$^{2+}$ provides an insight into the unique nature of a probable intermediate in both the evolution and oxidation of hydrogen.[96] Of particular interest is the short distance between the hydride and the proton in the NH cofactor. An essential $NH^{\delta+}\cdots H^{\delta-}$ interaction may be relevant to a small difference between the first and second protonation constants estimated at 10^2 in a CH_2Cl_2 solution. Compared to [t-H-**39**]$^{+}$, the protonated [t-H-**39**^{H}]$^{2+}$ cation more slowly isomerizes to the μ-hydride. Probably, it is this dihydrogen interaction that stabilizes the terminal hydride.

For both the pdt and adt^{H} derivatives, the terminal hydrides are reduced at 100 – 200 mV more positive potentials than the corresponding bridging hydrides. The difference in the reduction potentials between the isomeric hydrides is proposed to reflect the differences in the localization of the electron upon reduction. In the case of the μ-hydride isomer, the reduction is likely to be more delocalized between two equivalent Fe centres. When the hydride is bound to one Fe atom, the reduction occurs at the Fe centre containing no hydride ligands. The crystallographic data reported by Carroll *et al.*[96] demonstrate how this reduction can induce the formation of a mixed-valence dihydrogen complex (Scheme 6).

Scheme 6



Scheme 6 underscores the role of electron transfer in the proton binding step in the hydrogen evolution reaction. Upon the reduction, the hydrogen evolution will produce a mixed-valence derivative similar to the H_{ox} state of the enzyme.

In HER catalyzed by [μ-H-**39**]$^{+}$, the starting complex **39** is not regenerated. Otherwise, an increase in the reaction rate would be observed due to the protonation of complex **39** giving the [t-H-**39**]$^{+}$ cation, which also serves as the active catalyst. Therefore, the authors concluded that the μ-hydride complexes are side products.[96] A related mechanism was invoked by Talarmin and co-workers[97] for the catalysis by the complex $[Fe_2(pdt)(\mu\text{-}H)(CO)_4(dppe)]^{+}$.

Although bioinspired complexes proposed by Carroll and co-workers are highly efficient proton reduction catalysts, a number of problems remain to be solved. These catalysts function at highly negative reduction potentials, resulting in high overpotentials. One possible solution is to construct a redox-active centre, which could mediate the electron transfer and facilitate the metal – hydride bond cleavage and the H – H bond formation.[98]

The incorporation of a synthetic catalyst into a protein or another macromolecule in order to construct the desired structure of the active site is a challenge. For example, Fe_2S_2 complex **41** was incorporated into the protein nitrobindin

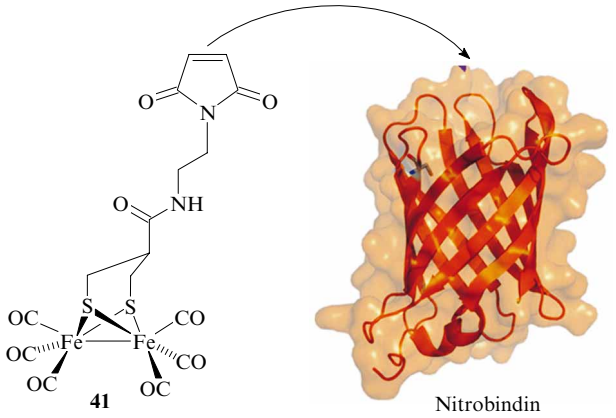


Figure 3. Schematic representation of the incorporation of complex **41** into nitrobindin.[99]

(Fig. 3).[99] Nitrobindin is a protein having a β-barrel structure, which usually binds a haem within a large inner cavity. The Fe_2S_2 complex was covalently embedded, instead of the haem, by linking the maleimide moiety to a Cys residue within the β-barrel (see Fig. 3). The activity of the hybrid catalyst in the H_2 evolution reaction induced by a photosensitizer is higher (TON = 130) than that of the Fe_2S_2 complex attached to peptides.[99] This system is also notable for the use of a stable covalent bond for attaching a catalyst to a polypeptide, as opposed to weaker coordination bonds utilized in peptide systems and hydrophobic interactions employed to attach catalysts to a photosystem.

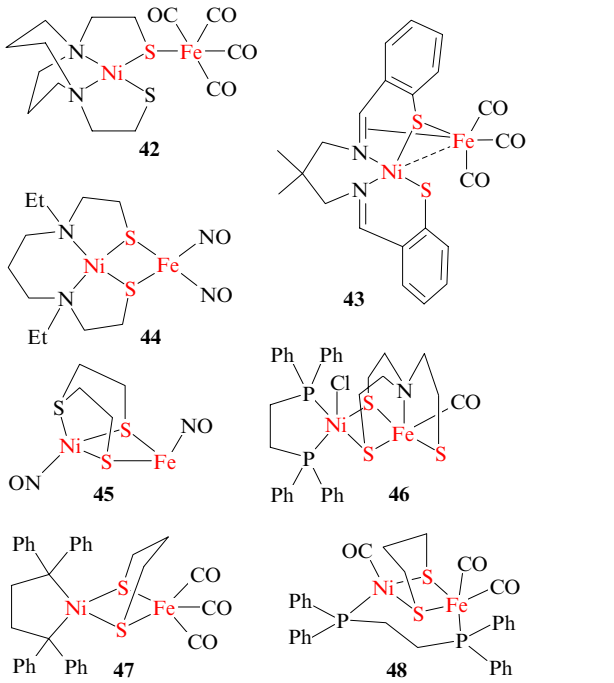
IV. Some structural analogues of [NiFe]-hydrogenases

The design of new structural analogues of [NiFe]-hydrogenases has attracted considerable interest after the publication of first X-ray diffraction data for the enzyme active site in 1995.[100] The structure of this enzyme continues to be extensively studied.[101–105] It was established that the active site of the enzyme contains both the Ni and Fe centres in different ligand environments. The distance between the metal centres is one of the most important parameters, which was extracted from X-ray diffraction data and which was employed to compare the new structural analogues with each other. The active site is sensitive to oxygen and consists of the heterodinuclear fragment $[(′S′)_2Ni(μ\text{-}′S′)_2(μ\text{-}X)Fe(CO)(CN)_2]$ (′S′ is cysteine, X = O or OH) (see structure **2**).[106]

The characteristic structural feature of these enzymes is that two metal centres are linked by an S bridge. Therefore, the most simple approach to the construction of structural analogues of the enzyme active site is based on the synthesis of a Ni complex with sulfur-containing chelating ligands and its subsequent use as a metallothiolate ligand for the Fe-metal centre.[107] This strategy for the preparation of new structural analogues of [NiFe]-hydrogenases is most commonly applied.

In 1996, Darensbourg and co-workers[108] characterized for the first time the structure of thiolate-bridged dinuclear carbonyl complex **42**. They demonstrated that the metallation of the nickel(II) complex containing the central NiN_2S_2 unit at the S atom using the iron carbonyl $[Fe_2(CO)_9]$ affords a stable heterobimetallic complex. In this case, the Ni complex acts as a monodentate ligand for the $\{Fe(CO)_4\}$ fragment. However, the distance between the Ni and Fe centres (3.76 Å) is much longer than that in the active site of the natural enzyme (2.6 – 2.9 Å). The reaction of the Ni^{2+} diimine dithiolate complex with $[Fe_2(CO)_9]$ produces dinuclear complex **43**, in which the coordination sphere of the iron atom is completed through the coordination by one of C=N π-bonds. The distance between the metal centres is 2.9 Å, thus enabling their potential interaction.[109] The first example of the dinuclear NiFe complex with two thiolate bridges (compound **44**) was described by Pohl and co-workers[110] in 1997. Due to the double bridge, the distance between the metal centres in the complex is 2.8 Å. In this case, the Fe atom is not coordinated by carbonyl ligands and has only two nitrosyl ligands. More recently, related complexes, *e.g.*, compound **45**, were synthesized.[111] Methods for the synthesis of exact structural analogues of hydrogenases, in which the Ni centre surrounded by four sulfur atom is linked by two bridges to the Fe centre coordinated by carbonyl and nitrile ligands, were progressively developed. Complex **46** is the first structural analogue with a double thiolate bridge and carbonyl ligands at the Fe centre; however, the distance between the metal centres in this complex (3.3 Å) is too long.[112,113] The coordination of soft phosphine ligands to the Ni centre resulted in the formation of complexes containing the metal centres at a distance of ~2.5 Å from each other, which ensures the Ni – Fe interaction observed in the active sites of the natural enzyme. For instance, complex **47** was synthesized by the reaction of [Ni(dppe)(pdt)] with $[Fe_3(CO)_{12}]$ or $[Fe(CO)_3(bda)]$ (bda is benzylideneacetone).[114] The distance between the metal centres corresponds to the distance in the natural enzymes. However, compound **47** is unstable and is transformed into complex **48**, in which the Ni – Fe distance is 2.48 Å, upon heating under reflux in benzene.

Structures 42 – 48



Several research teams studied dinuclear NiFe complexes containing a cyclopentadienyl moiety. For example, the reaction of [Ni(dppe)(pdt)] with [FeCp(CO)$_2$I] produces complex **49**, in which the Ni – Fe distance is 2.78 Å.[114]

In complex **50**, the Ni – Fe distance is also quite short (2.53 Å). In related complexes **51** and **52**, this distance is 3.17 Å.[115]

The next step was made by Sellmann *et al.*,[116] who synthesized complex **53** having a low-spin Ni^{II} centre, which is surrounded only by sulfur atoms and is linked to the low-spin Fe^{II} – CO fragment through two thiolate bridges. The CO(PMe$_3$)$_2$ environment around the Fe centre is similar to the CO(CN)$_2$ environment found for the Fe centre in the enzyme active site.

1,2-Bis(3,3-dimethyl-4-sulfanyl-2-thiabutyl)benzene (H$_2$xbsms)[117] is one of the promising ligands for the synthesis of [NiFe]-hydrogenase analogues. The reaction of the complex [Ni(xbsms)] with [Fe$_2$(CO)$_9$], [Fe(CO)$_2$(NO$_2$)] or [Fe(CO)$_4$I$_2$] produces the complexes [Ni(xbsms)Fe(CO)$_4$] (structurally similar to complex **42**), [Ni(xbsms)Fe(NO)$_2$] (structurally similar to complex **44**) and the new complex [Ni(xbsms)Fe(CO)$_2$I$_2$] (**54**), respectively.[118] The presence of the Ni(μ-S)$_2$Fe bridge in these complexes was established by spectroscopic methods; however, crystallographic data for these compounds are absent.

It was not until 2005, *i.e.*, 10 years after the determination of the enzyme structure, that several research groups synthesized and structurally characterized the closest analogue of the hydrogenase active site (complex **55**) containing the key structural unit, namely, the Fe centre surrounded only by CO and CN ligands.[119] This complex was prepared by the reaction of the Ni complexes with the pre-synthesized iron(II) complex [Fe(CO)$_3$(CN)$_2$Br]$^-$. In complex **55**, the Ni – Fe distance is 3.05 Å and the Fe – S – Ni angle is 85°, which, on the whole, correspond to the parameters of the oxidized form of [NiFe]-hydrogenase. However, the coordination environment of the Ni centre in complex **55** has a square planar geometry unlike the strongly distorted geometry of the NiS$_4$ unit found in different forms of the enzymes.

Therefore, there are a few successful examples of structural analogues of [NiFe]-hydrogenases. Strange as it may seem, none of the described analogues was used as the catalyst for hydrogen oxidation or proton reduction to hydrogen.

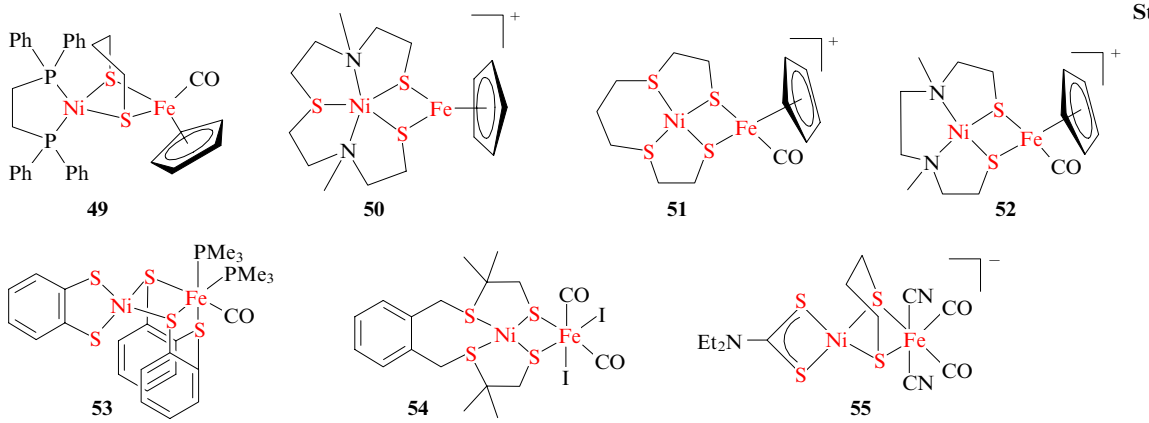
V. Functional analogues of [NiFe]-hydrogenases

As can be seen from the data presented in the previous section, the number of characterized structural analogues is much larger than the number of functional dinuclear analogues of [NiFe]-hydrogenases, *i.e.*, those exhibiting considerable catalytic activity in hydrogen oxidation and proton reduction reactions.

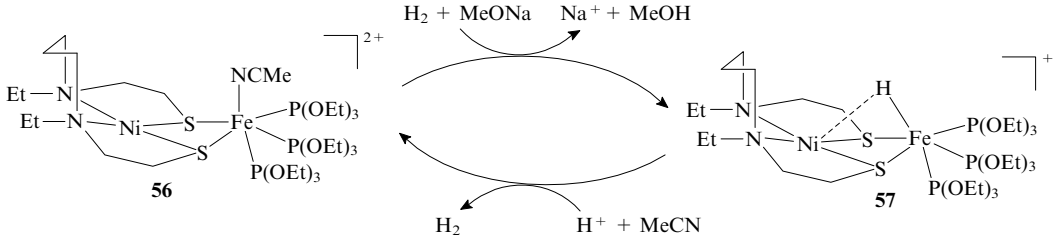
Ogo's research team[120] synthesized the new complex [Ni(L)Fe(MeCN){P(OEt)$_3$}$_3$](BPh$_4$)$_2$ (**56**) (L is *N*,*N*′-diethyl-3,7-diazanonane-1,9-dithiolate), which most closely resembles the structural features of [NiFe]-hydrogenases. The reaction of this complex with hydrogen in the presence of a strong base (MeONa) gives hydride complex **57**, which generates molecular hydrogen and is transformed into complex **56** when reacting with a proton (Scheme 7). Therefore, this is the first NiFe complex that mediates both the hydrogen oxidation and proton reduction to hydrogen, *i.e.*, this complex is simultaneously the structural and functional hydrogenase analogue.[120]

Trinuclear complex **58** is the only NiFe$_2$ complex exhibiting catalytic activity in the electroreduction of protons to hydrogen.[121] In this diamagnetic complex, the distance between the Fe centres is 2.66 Å and the distance between Ni and Fe is 2.50 Å, which enable the Fe – Fe and Fe – Ni interactions, respectively. The coordination environment of the Ni atom is formed by four S atoms and two Fe atoms and has a distorted octahedral geometry. Voltammetric

Structures 49 – 55



Scheme 7



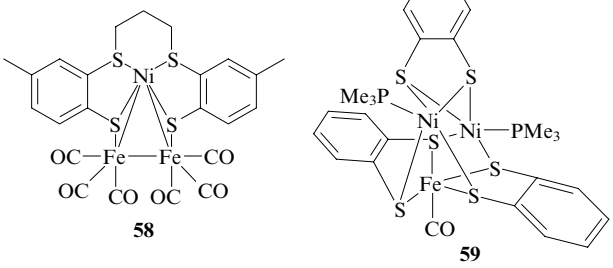
measurements for complex **58** demonstrated a reversible one-electron reduction at a potential of −1.03 V. The addition of trifluoroacetic acid as a proton donor to a solution of complex **58** in CH_2Cl_2 led to a considerable cathodic current increase in the cyclic voltammogram that was directly proportional to the acid concentration in solution. Moreover, at a potential of −1.64 V, complex **58** catalyzes the reduction of trifluoroacetic acid to hydrogen with a turnover number of up to 6 h^{-1}. In the presence of the acid, the catalyst is stable for 1 h and then it decomposes. The catalytic process involves the one-electron reduction of complex **58** followed by the proton attachment most likely to the metal centre or at the midpoint between the metal centres rather than to sulfur atoms in the reduced form $[H\text{-}\mathbf{58}]^-$ and evolution of molecular hydrogen.

Trinuclear Ni_2Fe complex **59**, in which the metal centres are surrounded mainly by sulfur atoms, was prepared by Sellmann *et al.*[122] in 2004 as one of the first functional analogues of [NiFe]-hydrogenases. However, the relevant data on the catalytic activity of the complex were not reported. It was only demonstrated that the treatment of diamagnetic complex **59** with tetrafluoroboric acid (HBF_4) leads to the oxidation of the complex to the state $(\mathbf{59})^+$ accompanied by evolution of molecular hydrogen, as was detected by ^1H NMR spectroscopy. The redox transfer $\mathbf{59}/(\mathbf{59})^+$ is reversible and occurs at 0.095 V *versus* the SHE in methylene chloride. However, this complex exhibited weak catalytic activity in the bulk electrolysis (the turnover number is 0.1 h^{-1}).[123]

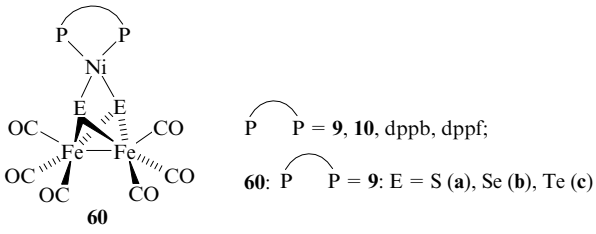
Hence, due to the presence of several pair interactions between the metal centres in complexes **58** and **59**, as well as owing to high stability of the forms $(\mathbf{58})^-$ and $(\mathbf{59})$,$^+$ these complexes are potentially efficient catalysts for proton reduction to hydrogen. On the contrary, the absence of published data on the catalytic activity of dinuclear NiFe complexes suggests that these complexes are unstable in redox transformations that occur during the catalytic process.

New trinuclear cluster complexes of the general formula $(diphosphine)Ni(\mu_3\text{-}E)_2Fe_2(CO)_6$ **60** were synthesized by Song's research team[124] with the goal of estimating the influence of the chalcogen nature on their redox properties, as well as on the electrocatalytic efficiency in the hydrogen evolution reaction. Complexes **60a–c** exhibit a quasi-reversible reduction peak corresponding to the Fe^IFe^I/Fe^IFe^0 transition at potentials of −1.79, −1.71 and −1.62 V, respectively, and one a irreversible reduction peak corresponding Fe^IFe^0/Fe^0Fe^0 transitions at potentials of −1.96, −1.95 and −1.92 V, respectively. Therefore, in the series of S → Se → Te, the reduction potential is shifted towards less negative values. Two one-electron oxidation peaks at potentials of −0.01 to 0.15 V correspond to $Fe^IFe^I/Fe^IFe^{II}/Fe^{II}Fe^{II}$ transitions. The third oxidation peak at potentials of 1.04, 0.94 and 0.92 V for complexes **60a–c**, respectively, is assigned to the Ni^{II}/Ni^{III} transition. Complexes of the general formula $(diphosphine)Ni(\mu_3\text{-}E)_2Fe_2(CO)_6$ [diphosphine is dppv, dppe, 1,4-bis(diphenylphosphino)butane (dppb), 1,1′-bis(diphenylphosphino)ferrocene (dppf)] display electrocatalytic properties in the hydrogen evolution reaction in the presence of TsOH as the proton donor in MeCN. The turnover number for these complexes was 7.8–8.8 in 0.5 h. The potentials of catalytic hydrogen evolution (−1.73, −1.69 and −1.68 V for compounds **60a–c**, respectively) also correlate with the chalcogen nature in the trinuclear complex.[124]

Structures 58, 59

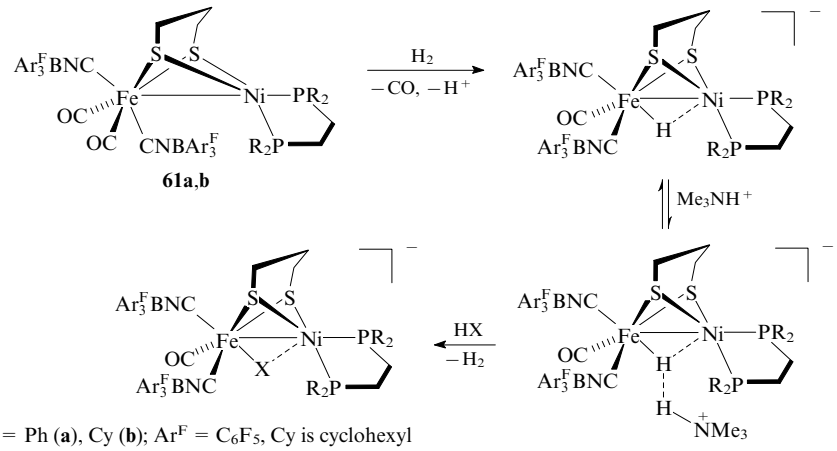


Structures 60



Rauchfuss's research team[125] synthesized complexes of the general formula $(CO)_2(CNBAr^F_3)_2Fe(\mu\text{-pdt})Ni(dxpe)$ [dxpe = dppe or dcpe, dcpe is 1,2-bis(dicyclohexylphosphino)ethane] (**61a**,**b**), in which two CO groups and two BAr^F_3 moieties serve for the protection of cyano groups at the Fe atom (Scheme 8). Besides, the introduction of the BAr^F_3

Scheme 8



R = Ph (**a**), Cy (**b**); $Ar^F = C_6F_5$, Cy is cyclohexyl

group results in an increase in the electrophilicity of the Fe centre, thus facilitating hydrogen activation.[126]

Scheme 8 shows the mechanism of hydrogen activation in the coordination sphere of the NiFe complex giving intermediate hydrides, which can again eliminate hydrogen in the presence of the added acids.

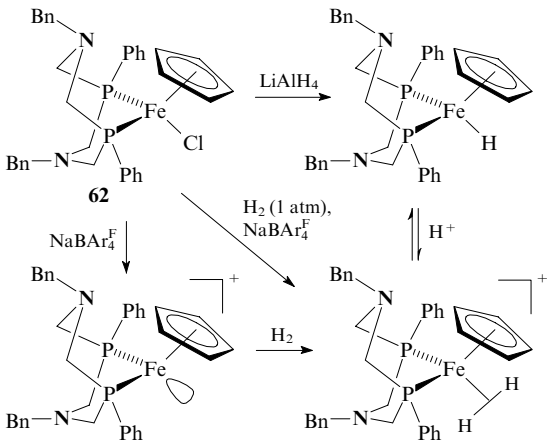
VI. Iron complexes for hydrogen oxidation

Iron complexes containing pendant N-bases in the ligands were thoroughly investigated in the hydrogen oxidation reaction.[127–130] The presence of pendant amino groups in the ligands can substantially increase the H_2 oxidation rate, as demonstrated in studies of nickel complexes.[35–38, 131–133] These amino groups not only mediate intra- and intermolecular proton transfer reactions but also provide additional advantages. Thus, they facilitate the binding and heterolytic cleavage of an H_2 molecule in such a way that the hydride is linked to the metal atom and the proton is attached to the pendant amino group. Bullock and co-workers[127–130] proposed fundamental principles required for the rational design of molecular electrocatalysts in relation to nickel complexes with diazadiphosphacyclooctanes $[Ni(P_2^RN_2^{R'})_2]^{2+}$ and applied these principles to iron complexes. A substantial difference of iron complexes is that Fe complexes with H_2 are more stable.

The complexes $[Ni(P_2^RN_2^{R'})_2]^{2+}$ serve as very active catalysts for H_2 evolution[131–138] and its oxidation.[139–142] Catalysts which are active both in the H_2 evolution and its oxidation,[143, 144] *i.e.*, dual-purpose catalysts, contain the cyclic 1,5-diaza-3,7-diphosphaoctane ligand $P_2^RN_2^{R'}$. The key feature of these catalysts is the presence of a pendant amine at a certain position, which functions as a proton relay in close proximity to a vacant coordination site of the redox-active metal centre, thus leading to bifunctional activation of H_2 during heterolytic cleavage or to the H – H bond formation. The efficient bifunctional activation requires the control of the hydride acceptor ability of the metal centre and the proton acceptor ability of the pendant base; it is these properties that are responsible for the ability of these catalysts to oxidize H_2, produce H_2 or perform catalysis in both directions.

Due to the presence of a vacant orbital on the Fe centre in the $[CpFe(P_2^{Ph}N_2^{Bn})]^+$ cation derived from complex **62** (Scheme 9), this cation reacts with hydrogen to form the complex $[CpFe(P_2^{Ph}N_2^{Bn})(H_2)]^+$. When reacted with a base and hydrogen, complex **62** is involved in subsequent steps of the catalytic cycle of hydrogen oxidation (binding of an H_2 molecule, its splitting, electrochemical oxidation and proton transfer). However, the catalytic activity is not observed in the hydrogen oxidation reaction. A more detailed investigation of the complex revealed the cause of its inefficiency, namely, a too weak interaction between the metal centre and the pendant base. Therefore, the modification of the catalyst structure was required in order to prepare a catalytically active complex. The phenyl substituent at the phosphorus atom was replaced by the bulky Bu^t group to ensure the interaction between the iron and nitrogen atoms; the cyclopentadienyl moiety containing the electron-withdrawing group C_6F_5 (complex **63a**) was introduced to increase the acidity of the H_2 ligand. Actually, all structural modifications of the iron complex resulted in the appearance of catalytic activity in the H_2 oxidation reaction. The catalytic current increase was observed at a potential of −0.8 V, the turnover frequency of the catalytic cycle was 2.0 s^{-1}, the overpotential was 0.16 V using *N*-methylpyrrolidine as a base (Table 5). The introduction of the tetrafluoropyridyl group possessing even stronger electron-withdrawing properties into the cyclopentadienyl moiety led to an increase in TOF for catalyst **63b** to 2.5 s^{-1} with an overpotential of 0.23 V under similar conditions.[127, 130]

Scheme 9



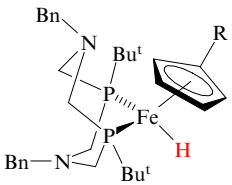
Certain differences in the catalytic properties are observed also for Fe complexes with PNP and P_2N_2 ligands. Thus, the turnover frequency of the catalytic cycle for the complex $Cp'Fe[P^{Et}N(Me)P^{Et}](H)$ [**64**, $Cp' = (4\text{-}C_5F_4N)C_5H_4$] (8.6 s^{-1}, see Table 5) is higher compared to the analogous complex with the P_2N_2 ligand; however, this improvement is accompanied by an increase in the overpotential to 0.41 V in the presence of *N*-methylpyrrolidine as a base. The reversible reduction peak of complex **64** is observed at more positive potentials compared to the analogous complex with the $P_2^RN_2^{R'}$ ligand, and the reversibility of the reduction peak is indicative of a slow proton transfer step. The experimental and theoretical data suggest that the proton transfer from the Fe atom to the N atom and subsequent deprotonation of the basic centre are the slow steps in the catalytic cycle.[127, 130]

The introduction of additional basic groups into the outer coordination sphere of the complex $Cp'Fe(P^{Et}N\{(CH_2)_3NMe_2\}P^{Et})(H)$ (**65**) leads to an increase in TOF to 290 s^{-1} without an increase in the overpotential (see Table 5). Theoretical calculations demonstrated that this effect was achieved due to the ability of protons to hop from the metal centre to the nearest amino group in the second coordination sphere and then to the most remote one in the outer sphere, from which the deprotonation occurs under the action of a base.[127, 130]

Table 5. Electrocatalytic data for complexes **63**–**65** in the hydrogen oxidation reaction in the presence of *N*-methylpyrrolidine as a base.[127, 130]

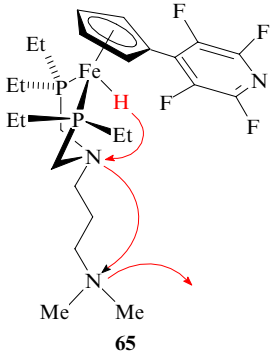
Complex	TOF /s^{-1}	Overpotential /mV
63a	2	160
63b	2.5	235
64	8.6	410
65	290	410

Structures 63 – 65

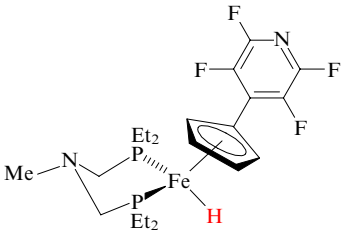


63a,b

R = C_6F_5 (**a**), 4-C_5F_4N (**b**)



65



64

VII. Assessment of the efficiency of homogeneous electrocatalysts

Molecular electrocatalysts for H_2 evolution are usually studied under various conditions (solvent and a proton source), which prevents the direct comparison of their activity. Savéant and Artero [145] proposed the most rational benchmarking based on the analysis of the current – potential response for two-electron two-step mechanisms and the derivation of catalytic Tafel plots reflecting the relationship between TOF and the overpotential based on the intrinsic properties of the catalyst independent of characteristics of the electrochemical cells.

In molecular electrocatalysis, the turnover frequency of the catalytic cycle is a kinetic parameter, which reflects the catalytic activity and depends on the applied potential. Savéant and Artero [145] noted that the complete picture of the catalytic properties can be got by determining the TOF values only from reactions at the surface of the electrode. In many reports, the TOF values were simply equated with the observed rate constant (k_{obs}) for catalyst regeneration, which can often be estimated from the plateau current in the cyclic voltammogram measured under pure kinetic conditions (without diffusion limitations) and no substrate consumption zone. This is a limiting value wherein TOF is constrained by the potential-independent rate constant k_{obs} and is taken as TOF_{max}.[41, 145 – 149]

In the region of CV, where the catalytic current has not yet reached its plateau, TOF is dependent on the applied potential (E) and reflects the percentage of the activated catalyst. In cases where all electron transfers are Nernstian, this relationship is described by Eqn (1):[145, 148 – 150]

$$TOF = \frac{TOF_{max}}{1 + \exp[F/RT\,(E - E_{cat/2})]} \qquad (1)$$

where F is the Faraday constant and R is the universal gas constant. When the applied potential is substantially more negative than the half-wave potential of the steady-state catalytic wave ($E_{cat/2}$), at which 50% of the catalyst is activated, Eqn (1) shows that TOF becomes independent of the overpotential and reaches the TOF_{max} value.

Equation (1) can be rewritten by including the overpotential to obtain the meaningful TOF – η relationship [Eqn (2)].[145]

$$TOF = \frac{TOF_{max}}{1 + \exp[F/RT\,(E^{\circ}_{A/B} - E_{cat/2})]\exp(-F\eta/RT)} \qquad (2)$$

where $E^{\circ}_{A/B}$ is the standard potential for substrate conversion.

The ECCE mechanism, in which the second electron transfer is more difficult than the first one, is the only exception from the general application of Eqs (1) and (2). In this case, the plot of TOF *versus* the applied potential is described by Eqn (3), where α is the transfer coefficient, which reflects the fact that the second electron transfer step is a dissociative electron-transfer reaction and does not obey the Nernst law.[149]

$$TOF = \frac{TOF_{max}}{1 + \exp[\alpha F/RT\,(E - E_{cat/2})]} \qquad (3)$$

In another exception, defined in the literature as a homolytic process, the TOF – η relationship is described by Eqn (4) and corresponds to a second-order chemical step (with respect to the catalyst).[149]

$$TOF = \frac{TOF_{max}}{\{1 + \exp[F/RT\,(E - E_{cat/2})]\}^{3/2}} \qquad (4)$$

The TOF – η relationship proposed by Savéant provides a tool for comparing the catalysts at different overpotentials. As can be seen from Eqn (2), which includes the standard potential for substrate conversion $E^{\circ}_{A/B}$, $TOF = 0.5\,TOF_{max}$ (for the homolytic process, $0.35\,TOF_{max}$) at the applied potential $E = E_{cat/2}$ (at the overpotential $E^{\circ}_{A/B} - E_{cat/2}$).[149, 150] As mentioned above, the potential-dependent region reflects the percentage of the active catalyst. For the general cases, the slope of this region of the plot equals to $F/(RT\ln 10)$. For the ECCE reaction scheme, in which the second electron transfer is more difficult than the first one, the slope is $\alpha[F/(RT\ln 10)]$, while for a homolytic reaction, the slope is $3F/(2RT\ln 10)$.[145]

Figure 4 illustrates the result of applying Eqn (2) to two catalysts with different $E^{\circ}_{P/Q}$ (the formal reduction potential of the catalyst P that is converted to the form Q) and k_{obs} (TOF_{max}) values and reducing the same substrate. These TOF – η plots provide for a means of assessing the potentials for a specific catalytic transformation at which different catalysts will be most useful. For instance, η for electrolysis can be optimized or the desired TOF can be achieved.[145]

It was also proposed the TOF^0 value obtained by the extrapolation of TOF to $E = E^{\circ}_{A/B}$.[145, 146, 149] For the general cases, this relationship is described by Eqn (5).

$$TOF^0 = TOF_{max}\exp\left[-\frac{F}{RT}(E^{\circ}_{A/B} - E_{cat/2})\right] \qquad (5)$$

Although TOF^0 was supposed for the assessment of which catalyst is good or bad in its nature,[149] it was noted that, since TOF^0 is dependent on the overpotential zero position, opposite results can be obtained by using substrates with different $E^{\circ}_{A/B}$ values.[151] Summary Table 6

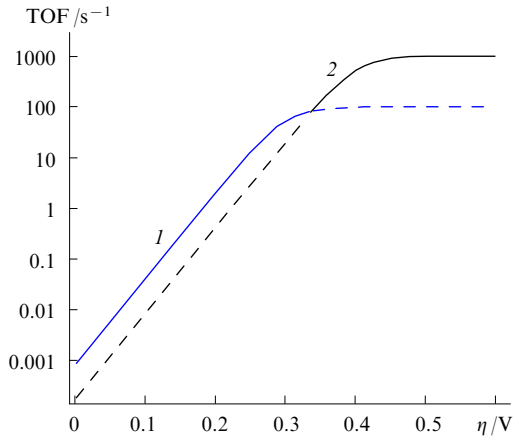


Figure 4. Plots of TOF *versus* the applied potential for two catalysts with different k_{obs} and $E^{\circ}_{P/Q}$ values.[145]
The zero potential intercept ($\eta = 0$) gives TOF^0; at the plateau, TOF = k_{obs}. The solid region lines indicate which catalyst has a higher TOF at a particular overpotential: catalyst *1* has a larger TOF^0, while catalyst *2* has a higher TOF$_{max}$. (*1*): $k_{obs} = 100$ s^{-1}, $E^{\circ}_{P/Q} = -0.3$ V; (*2*): $k_{obs} = 1000$ s^{-1}, $E^{\circ}_{P/Q} = -0.4$ V.

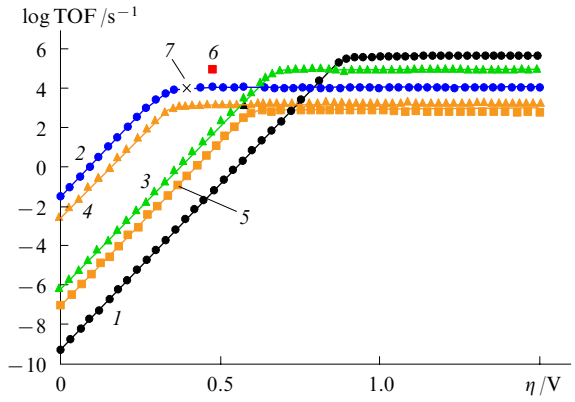


Figure 5. Catalytic Tafel plots logTOF – η for a series of iron, cobalt and nickel complexes (the solvent and acid are given in parentheses).
(*1*) Complex **66** (DMF, Et_3NH^+); (*2*) complex **67** (DMF, Et_3NH^+); (*3*) complex **68** (MeCN, $DMFH^+$); (*4*) complex **69a** (MeCN, $DMFH^+$); (*5*) complex **69b** (MeCN, TfOH);[145] (*6*) [t-H-**39**^{H}]$^{2+}$ (MeCN, CF_3CO_2H);[96] (*7*) complex **70** (MeCN, $DMFH^+$).[131]

gives the main catalytic parameters for a number of recently synthesized iron complexes with a different ligand environment.

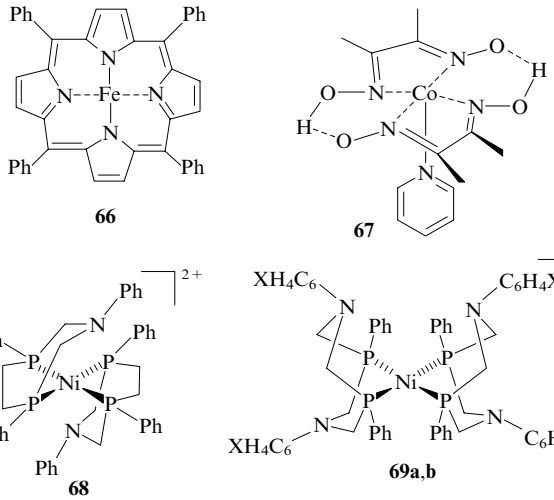
Besides, as mentioned above, the slope of the TOF – η plot may depend on the mechanism of the process, resulting in a serious distortion of estimates based on TOF^0. The TOF^0 value does not account for the possibility that substrates with different $E^{\circ}_{A/B}$ values may accelerate or slow down the homogeneous rate-limiting step, thus changing the rate of the catalysis. In addition, the TOF^0 value depends on the substrate concentration. Thus, the TOF^0 values changed by three orders of magnitude for a system, in which the substrate concentration changed by two orders of magnitude.[149] This inherent dependence of TOF^0 on both the nature of the substrate and its concentration underscores the necessity of comparing the catalysts at their identical concentrations using the same substrates at equal concentrations. It is unlikely that the catalysts described in the literature will be studied using substrates of the same nature at equal concentrations, *i.e.*, this parameter is useful only for tests in strictly definite cases, for instance, in a special comparative study of catalysts.

Although the kinetic parameters (k_{obs}, TOF$_{max}$ and the TOF – η plot) are valuable ones, their absolute values are not, in our opinion, the most significant characteristics for benchmarking, since it often depends on the conditions (for example, on the substrate concentration). Information about the mechanism of the process, which can be derived from the analysis of the reaction kinetics, is more important. This information can be used to derive the rate or rate constant law, *i.e.*, the law for the parameters providing a more unbiased estimate of the catalyst performance.

Good electrocatalysts are characterized by high TOF values at a low overpotential (see Figs 4 and 5). In other words, catalysts exhibiting high TOF at the expense of large overpotentials will not allow for a good power-to-chemical conversion yield, while those showing low catalytic rates, even near the thermodynamic equilibrium, will not enable the development of powerful electrocatalytic devices for electric power production in solar and fuel cells. Catalytic Tafel plots provide a unified approach ensuring that these two properties are observed simultaneously. The best catalysts are characterized by the curves that appear in the top left corner of these graphs.

This rational benchmarking of homogeneous H_2 evolution catalysts using catalytic Tafel plots, which properely relate the defined TOF value to the overpotential, allows one to compare the catalysts regardless of the character-

Structures 67 – 70



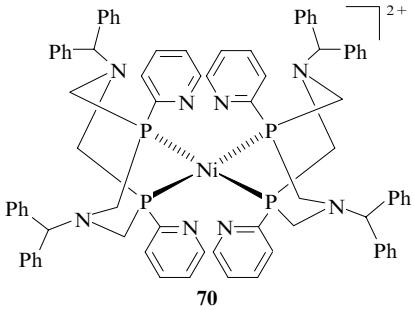
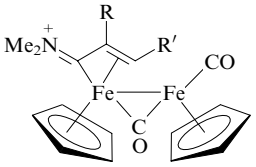


Table 6. Summary table of catalytic characteristics for selected iron complexes with a different ligand environment.

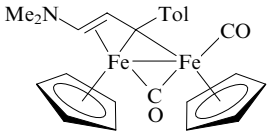
Complex	Proton source, solvent	E_p^{cat}, catalytic efficiency: TOF (s^{-1}), and(or) TON, and(or) faradaic yield (%)	Overpotential /V	Ref.
$Fe(Br_2Gm)_3(Bn\text{-}C_4H_9)_2$ (**37a**) (Gm is glyoxime)	$HClO_4$, MeCN	−0.75 V, 19%	0.49	57
[(μ-pdt)$Fe_2(CO)_4(\kappa^2$-bipy)] (**18**)	AcOH, MeCN	−2.06 V, 0.44 – 0.25	0.68	73
(μ-$SCH_2CH_2CH_2S$)[$Fe(CO)_3$]$_2$ (**26a**) (μ-SCH_2CH_2S)[$Fe(CO)_3$]$_2$	HOTs, HOAc, MeCN	–	0.44 – 0.71	29, 152
μ-(SCH(Me)CH_2S)$Fe_2(CO)_6$ μ-(SCH(Me)CH(Me)S)$Fe_2(CO)_6$ μ-(SCH_2CH(CH_2OH)S)$Fe_2(CO)_6$	4-Bu^tC_6H_4OH, MeCN	−2.2 V, weak current growth (20%)	0.40 – 0.75	153
$Fe_2S_2(CO)_6(NC_6H_4Br)$ (**35**)	H_2SO_4, H_2O	6400 s^{-1}, $\gg 10^8$, 95%	–	93
Dinuclear iron complexes **71a – c**, **72**, **73a – c**, **74a**,**b**, **75 – 78**	HOAc, MeCN	0.34 – 2.04 V, 15.5%	0.58	56
$Fe_2(adt^H)(CO)_2(dppv)_2$ (**39**) $Fe_2(pdt)(CO)_2(dppv)_2$ (**40**)	$HBF_4 \cdot Et_2O$, MeCN	4 – 58 000 s^{-1}	0.5 – > 1	96
[($P_2^{Ph}N_2^{Ph}$)Fe(Cp*)H], [($P_2^{Cy}N_2^{Ph}$)Fe(Cp*)H] (Cp* = C_5Me_5)	Tf_2NH, PhF	−1.4 V, complexes are unstable in acidic medium	–	154

Note.

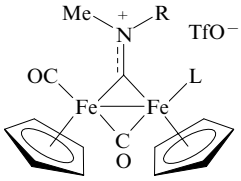


71a – c

R = H: R′ = Tol (**a**), CH_2OH (**b**);
R = SPh, R′ = CH_2OH (**c**);
Tol = 4-MeC_6H_4

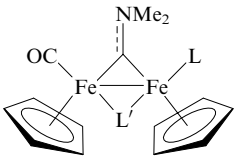


72



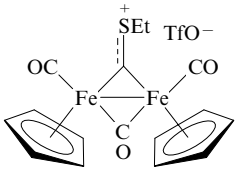
73a – c

R = Me: L = CO (**a**),
NCMe (**b**); R = 2,6-$Me_2C_6H_3$,
L = CO (**c**)

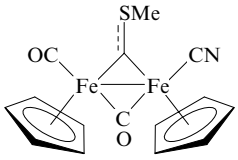


74a,**b**

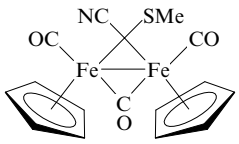
L = CN, L′ = CO (**a**);
L = CO, L′ = H (**b**)



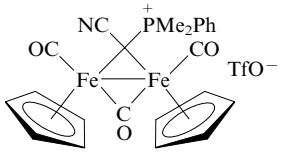
75



76



77



78

istics of a particular electrochemical cell and makes it possible to assess catalysts under different experimental conditions (solvent, proton donor), that is, without defining the standard measurement conditions.[147] Such plots are most conveniently derived by means of non-destructive techniques, *i.e.*, those providing information about the system without causing its damage (*e.g.*, cyclic voltammetry), and then these plots can be used to optimize the preparative-scale conditions, striking the balance between the speed and the energy consumption. This approach should be supplemented by catalyst stability testing.

In Fig. 5, the plots proposed by Savéant and Artero[145] are supplemented by the data for the best, based on certain parameters, hydrogenase analogues. Thus, [t-H-**39**^{H}]$^{2+}$, which is a leader based on TOF (58 000 s^{-1}) among analogues of [FeFe]-hydrogenases,[96] resides in the top left corner of the plot, because it functions at a relatively low overpotential (0.5 V) (point *6* in Fig. 5). Some nickel complexes with diazadiphosphacyclooctane ligands are also highly efficient catalysts, particularly those containing the 2-pyridyl substituent at the phosphorus atom and the $CHPh_2$ group at the nitrogen atom (TOF is 15 200 s^{-1} at an overpotential of 0.4 V) (point *7* in Fig. 5).[131] Therefore, the approach proposed by Savéant allows for a comparison of the activity of various metal complex catalysts for hydrogen evolution that are reduced at different potentials and function in different media.

VIII. Conclusion

The development of new biomimetic catalytic systems mimicking the action of metalloenzymes and biological nanoreactors (hydrogenases, oxidases, methyl-S-coenzyme M methyl reductases) is based on cage structures, which contain P, N and S donor atoms coordinated to iron atoms and form cavities composed of macrocycles and redox-active, also known as non-innocent, ligands in the second coordination sphere. A comparison of the activity and redox properties of mononuclear and dinuclear iron complexes with a similar ligand environment is important for an understanding of the mechanisms of catalytic transformations, as well as for the determination of the factors

responsible for the reactivity of the catalysts. Catalysts based on earth-abundant metals, which can replace platinum in fuel cells and function in hydrogen oxidation and evolution reactions, are of particular interest. Non-toxic iron is most attractive among these metals. Investigations of model complexes led to remarkable advances in understanding of how iron-containing hydrogenases function and, in some cases, allowed researchers to achieve the catalytic efficiency in hydrogen evolution and oxidation reactions comparable to natural enzymes in terms of the turnover number per second. Variations of the nature of substituents in different ligands and of dithiolate groups in iron complexes is one of the ways of tuning the catalytic properties of hydrogenase models. The search for more efficient and stable catalysts for electrochemical proton reduction to hydrogen and for the hydrogen oxidation involving different ligand platforms is ongoing since the problems, particularly those associated with the need of catalysts with low overpotentials and the use of aqueous solutions as sources of hydrogen, are still urgent issues. In recent years, a great progress has been achieved in engineering of bioinspired catalysts and assemblies of synthetic catalysts and biomolecules. The incorporation of a synthetic catalyst into a protein or another macromolecule to reproduce the desired structure of the active site of the enzyme is a challenge. Electrochemical methods play an important role in the determination of the mechanisms of biomimetic reactions. Indeed, these techniques are employed in almost every serious interdisciplinary research on the design of catalysts and the development of processes and materials associated with the charge transfer and redox reactions.[155 – 166]

Recently, the rational benchmarking of homogeneous H_2 evolution catalysts was proposed based on catalytic Tafel plots, which properly relate the defined turnover frequency to the overpotential. This allows for a comparison of catalysts regardless of the characteristics of a particular electrochemical cell and the estimation of their activity under distinct experimental conditions. As a rule, for the already known complexes, the lower the overpotential for hydrogen evolution, the lower the efficiency, while it is necessary to find such structural analogues of hydrogenases which would combine high activity, high TOF and TON values and low overpotentials.

Apparently, further extensive research will be aimed at solving problems, such as the development of new synthetic approaches to the control of the efficiency of biomimetic catalytic systems based on iron in different oxidation states in hydrogen evolution and oxidation reactions, investigation of the nature, chemical and electrochemical reactivity of intermediates, primarily protonated ones, and subsequent use of the results in processes of practical value for hydrogen power engineering and actual fuel cells.

This review has been written with the financial support of the Russian Foundation for Basic Research (Project No. 16-03-00195).

References

1. N S Lewis, D G Nocera *Proc. Natl. Acad. Sci. USA* **103** 15729 (2006)
2. H B Gray *Nat. Chem.* **1** 7 (2009)
3. A Thapper, S Styring, G Saracco, A W Rutherford, B Robert, A Magnuson, W Lubitz, A Llobet, P Kurz, A Holzwarth, S Fiechter, H de Groot, S Campagna, A Braun, H Bercegol, V Artero *Green* **3** 43 (2013)
4. D V Esposito, S T Hunt, A L Stottlemyer, K D Dobson, B E McCandless, R W Birkmire, J G Chen *Angew. Chem., Int. Ed.* **49** 9859 (2010)
5. M Rakowski DuBois, D L DuBois *Acc. Chem. Res.* **42** 1974 (2009)
6. V Artero, M Chavarot-Kerlidou, M Fontecave *Angew. Chem., Int. Ed.* **50** 7238 (2011)
7. M Wang, L Chen, L Sun *Energy Environ. Sci.* **5** 6763 (2012)
8. N Queyriaux, R T Jane, J Massin, V Artero, M Chavarot-Kerlidou *Coord. Chem. Rev.* **304 – 305** 3 (2015)
9. R H Crabtree *New J. Chem.* **35** 18 (2011)
10. V S Thoi, H I Karunadasa, Y Surendranath, J R Long, C J Chang *Energy Environ. Sci.* **5** 7762 (2012)
11. Y Sun, J P Bigi, N A Piro, M L Tang, J R Long, C J Chang *J. Am. Chem. Soc.* **133** 9212 (2011)
12. L Chen, M Wang, K Han, P Zhang, F Gloaguen, L Sun *Energy Environ. Sci.* **7** 329 (2014)
13. M L Helm, M P Stewart, R M Bullock, M Rakowski DuBois, D L DuBois *Science* **333** 863 (2011)
14. J C Fontecilla-Camps, A Volbeda, C Cavazza, Y Nicolet *Chem. Rev.* **107** 4273 (2007)
15. W Lubitz, H Ogata, O Rüdiger, E Reijerse *Chem. Rev.* **114** 4081 (2014)
16. K A Vincent, A Parkin, F A Armstrong *Chem. Rev.* **107** 4366 (2007)
17. R Cammack *Nature (London)* **397** 214 (1999)
18. E C Hatchikian, N Forget, V M Fernández, R Williams, R Cammack *Eur. J. Biochem.* **209** 357 (1992)
19. C Bolm *Nat. Chem.* **1** 420 (2009)
20. T R Simmons, V Artero *Angew. Chem., Int. Ed.* **52** 6143 (2013)
21. I Bhugun, D Lexa, J-M Savéant *J. Am. Chem. Soc.* **118** 3982 (1996)
22. M J Rose, H B Gray, J R Winkler *J. Am. Chem. Soc.* **134** 8310 (2012)
23. T Liu, D L DuBois, R M Bullock *Nat. Chem.* **5** 228 (2013)
24. S V Hexter, F Grey, T Happe, V Climent, F A Armstrong *Proc. Natl. Acad. Sci. USA* **109** 11516 (2012)
25. V Fourmond, C Greco, K Sybirna, C Baffert, P-H Wang, P Ezanno, M Montefiori, M Bruschi, I Meynial-Salles, P Soucaille, J Blumberger, H Bottin, L De Gioia, C Léger *Nat. Chem.* **6** 336 (2014)
26. E J Lyon, I P Georgakaki, J H Reibenspies, M Y Darensbourg *Angew. Chem., Int. Ed.* **38** 3178 (1999)
27. A Le Cloirec, S C Davies, D J Evans, D L Hughes, C J Pickett, S P Best, S Borg *Chem. Commun.* 2285 (1999)
28. M Schmidt, S M Contakes, T B Rauchfuss *J. Am. Chem. Soc.* **121** 9736 (1999)
29. C Tard, X Liu, S K Ibrahim, M Bruschi, L De Gioia, S C Davies, X Yang, L-S Wang, G Sawers, C J Pickett *Nature (London)* **433** 610 (2005)
30. J-F Capon, F Gloaguen, F Y Pétillon, P Schollhammer, J Talarmin *Coord. Chem. Rev.* **253** 1476 (2009)
31. G A N Felton, C A Mebi, B J Petro, A K Vannucci, D H Evans, R S Glass, D L Lichtenberger *J. Organomet. Chem.* **694** 2681 (2009)
32. B E Barton, M T Olsen, T B Rauchfuss *Curr. Opin. Biotechnol.* **21** 292 (2010)
33. T B Rauchfuss *Acc. Chem. Res.* **48** 2107 (2015)
34. J M Camara, T B Rauchfuss *Nat. Chem.* **4** 26 (2012)
35. G Berggren, A Adamska, C Lambertz, T R Simmons, J Esselborn, M Atta, S Gambarelli, J-M Mouesca, E Reijerse, W Lubitz, T Happe, V Artero, M Fontecave *Nature (London)* **499** 66 (2013)
36. S Ghosh, G Hogarth, N Hollingsworth, K B Holt, I Richards, M G Richmond, B E Sanchez, D Unwin *Dalton Trans.* **42** 6775 (2013)
37. N Wang, M Wang, L Chen, L Sun *Dalton Trans.* **42** 12059 (2013)
38. T R Simmons, G Berggren, M Bacchi, M Fontecave, V Artero *Coord. Chem. Rev.* **270 – 271** 127 (2014)

39. U-P Apfel, F Y Pétillon, P Schollhammer, J Talarmin, W Weigand, in *Bioinspired Catalysis* (Eds W Weigand, P Schollhammer) (Berlin: Wiley-VCH, 2014) p. 79
40. F Gloaguen, J D Lawrence, T B Rauchfuss, M Bénard, M-M Rohmer *Inorg. Chem.* **41** 6573 (2002)
41. F Gloaguen *Inorg. Chem.* **55** 390 (2016)
42. K Ye, Y-Y Li, R-Z Liao *RSC Adv.* **6** 90035 (2016)
43. D Chouffai, J-F Capon, L De Gioia, F Y Pétillon, P Schollhammer, J Talarmin, G Zampella *Inorg. Chem.* **54** 299 (2015)
44. M Bourrez, R Steinmetz, F Gloaguen *Inorg. Chem.* **53** 10667 (2014)
45. Yu G Budnikova *Sovremennyi Organicheskii Elektrosintez. Printsipy, Metody Issledovaniya i Prakticheskie Prilozheniya (Seriya 'Nauchnaya Mysl')* [Modern Organic Electrosynthesis. Principles, Methods of Investigation and Practical Applications (Series 'Scientific Idea')] (Moscow: Infra-M, 2016)
46. P Zanello *Inorganic Electrochemistry. Theory, Practice and Applications* (Cambridge: The Royal Society of Chemistry, UK, 2003)
47. B W Caplins, J P Lomont, S C Nguyen, C B Harris *J. Phys. Chem. A* **118** 11529 (2014)
48. M Mirmohades, S Pullen, M Stein, S Maji, S Ott, L Hammarström, R Lomoth *J. Am. Chem. Soc.* **136** 17366 (2014)
49. S Sicolo, M Bruschi, L Bertini, G Zampella, G Filippi, F Arrigoni, L De Gioia, C Greco *Int. J. Hydrogen Energy* **39** 18565 (2014)
50. B H Solis, S Hammes-Schiffer *Inorg. Chem.* **53** 6427 (2014)
51. S Raugei, D L DuBois, R Rousseau, S Chen, M-H Ho, R M Bullock, M Dupuis *Acc. Chem. Res.* **48** 248 (2015)
52. M Bourrez, F Gloaguen *New J. Chem.* **39** 8073 (2015)
53. Y C Lam, R J Nielsen, H B Gray, W A Goddard III *ACS Catal.* **5** 2521 (2015)
54. C Riplinger, E A Carter *ACS Catal.* **5** 900 (2015)
55. W P Fehlhammer, H Stolzenberg, in *Comprehensive Organometallic Chemistry* (Eds G Wilkinson, F G A Stone, E W Abel) (Oxford: Pergamon Press, 1982) p. 513
56. R Mazzoni, A Gabiccini, C Cesari, V Zanotti, I Gualandi, D Tonelli *Organometallics* **34** 3228 (2015)
57. A V Dolganov, A S Belov, V V Novikov, A V Vologzhanina, G V Romanenko, Yu G Budnikova, G E Zelinskii, M I Buzin, Ya Z Voloshin *Dalton Trans.* **44** 2476 (2015)
58. S Jiang, J Liu, Y Shi, Z Wang, B Åkermark, L Sun *Polyhedron* **26** 1499 (2007)
59. L-C Song, J-H Ge, X-F Liu, L-Q Zhao, Q-M Hu *J. Organomet. Chem.* **691** 5701 (2006)
60. D L DuBois, R M Bullock *Eur. J. Inorg. Chem.* 1017 (2011)
61. C Tard, C J Pickett *Chem. Rev.* **109** 2245 (2009)
62. D M Heinekey *J. Organomet. Chem.* **694** 2671 (2009)
63. F Gloaguen, T B Rauchfuss *Chem. Soc. Rev.* **38** 100 (2009)
64. J-F Capon, F Gloaguen, F Y Pétillon, P Schollhammer, J Talarmin *Eur. J. Inorg. Chem.* 4671 (2008)
65. L-C Song, Z-C Gu, W-W Zhang, Q-L Li, Y-X Wang, H-F Wang *Organometallics* **34** 4147 (2015)
66. F Gloaguen, J D Lawrence, T B Rauchfuss *J. Am. Chem. Soc.* **123** 9476 (2001)
67. R Mejia-Rodriguez, D Chong, J H Reibenspies, M P Soriaga, M Y Darensbourg *J. Am. Chem. Soc.* **126** 12004 (2004)
68. G A N Felton, A K Vannucci, J Chen, L T Lockett, N Okumura, B J Petro, U I Zakai, D H Evans, R S Glass, D L Lichtenberger *J. Am. Chem. Soc.* **129** 12521 (2007)
69. T Liu, M Y Darensbourg *J. Am. Chem. Soc.* **129** 7008 (2007)
70. S Ott, M Kritikos, B Åkermark, L Sun, R Lomoth *Angew. Chem., Int. Ed.* **43** 1006 (2004)
71. S Jiang, J Liu, Y Shi, Z Wang, B Åkermark, L Sun *Dalton Trans.* 896 (2007)
72. B E Barton, M T Olsen, T B Rauchfuss *J. Am. Chem. Soc.* **130** 16834 (2008)
73. S Roy, T L Groy, A K Jones *Dalton Trans.* **42** 3843 (2013)
74. T Yu, Y Zeng, J Chen, Y-Y Li, G Yang, Y Li *Angew. Chem., Int. Ed.* **52** 5631 (2013)
75. L-C Song, C-G Li, J Gao, B-S Yin, X Luo, X-G Zhang, H-L Bao, Q-M Hu *Inorg. Chem.* **47** 4545 (2008)
76. Y Na, M Wang, K Jin, R Zhang, L Sun *J. Organomet. Chem.* **691** 5045 (2006)
77. P Li, M Wang, L Chen, J Liu, Z Zhao, L Sun *Dalton Trans.* 1919 (2009)
78. L Duan, M Wang, P Li, Y Na, N Wang, L Sun *Dalton Trans.* 1277 (2007)
79. L-C Song, Z-Y Yang, H-Z Bian, Y Liu, H-T Wang, X-F Liu, Q-M Hu *Organometallics* **24** 6126 (2005)
80. L-C Song, J Gao, H-T Wang, Y-J Hua, H-T Fan, X-G Zhang, Q-M Hu *Organometallics* **25** 5724 (2006)
81. L-C Song, J-H Ge, X-G Zhang, Y Liu, Q-M Hu *Eur. J. Inorg. Chem.* 3204 (2006)
82. J-F Capon, F Gloaguen, P Schollhammer, J Talarmin *J. Electroanal. Chem.* **566** 241 (2004)
83. J-F Capon, F Gloaguen, P Schollhammer, J Talarmin *J. Electroanal. Chem.* **595** 47 (2006)
84. H Abul-Futouh, L R Almazahreh, T Sakamoto, N Y T Stessman, D L Lichtenberger, R S Glass, H Görls, M El-Khateeb, P Schollhammer, G Mloston,W Weigand *Chem. – Eur. J.* **23** 346 (2017)
85. J Chen, A K Vannucci, C A Mebi, N Okumura, S C Borowski, M Swenson, L T Lockett, D H Evans, R S Glass, D L Lichtenberger *Organometallics* **29** 5330 (2010)
86. D Schilter, J M Camara, M T Huynh, S Hammes-Schiffer, T B Rauchfuss *Chem. Rev.* **116** 8693 (2016)
87. O A Ulloa, M T Huynh, C P Richers, J A Bertke, M J Nilges, S Hammes-Schiffer, T B Rauchfuss *J. Am. Chem. Soc.* **138** 9234 (2016)
88. Y Na, M Wang, J Pan, P Zhang, B Åkermark, L Sun *Inorg. Chem.* **47** 2805 (2008)
89. Z Wang, J Liu, C He, S Jiang, B Åkermark, L Sun *Inorg. Chim. Acta* **360** 2411 (2007)
90. P Li, M Wang, L Chen, N Wang, T Zhang, L Sun *CrystEngComm* **10** 267 (2008)
91. C M Thomas, O Rüdiger, T Liu, C E Carson, M B Hall, M Y Darensbourg *Organometallics* **26** 3976 (2007)
92. M L Singleton, J H Reibenspies, M Y Darensbourg *J. Am. Chem. Soc.* **132** 8870 (2010)
93. S Dey, A Rana, S G Dey, A Dey *ACS Catal.* **3** 429 (2013)
94. D Zheng, M Wang, N Wang, M Cheng, L Sun *Inorg. Chem.* **55** 411 (2016)
95. A V Dolganov, I G Belaya, Ya Z Voloshin *Electrochim. Acta* **125** 302 (2014)
96. M E Carroll, B E Barton, T B Rauchfuss, P J Carroll *J. Am. Chem. Soc.* **134** 18843 (2012)
97. S Ezzaher, J-F Capon, N Dumontet, F Gloaguen, F Y Pétillon, P Schollhammer, J Talarmin *J. Electroanal. Chem.* **626** 161 (2009)
98. B Kandemir, S Chakraborty, Y Guo, K L Bren *Inorg. Chem.* **55** 467 (2016)
99. A Onoda, Y Kihara, K Fukumoto, Y Sano, T Hayashi *ACS Catal.* **4** 2645 (2014)
100. A Volbeda, M-H Charon, C Piras, E C Hatchikian, M Frey, J C Fontecilla-Camps *Nature (London)* **373** 580 (1995)
101. J Fritsch, P Scheerer, S Frielingsdorf, S Kroschinsky, B Friedrich, O Lenz, C M T Spahn *Nature (London)* **479** 249 (2011)
102. Y Shomura, K-S Yoon, H Nishihara, Y Higuchi *Nature (London)* **479** 253 (2011)
103. S P Best *Coord. Chem. Rev.* **249** 1536 (2005)
104. A L de Lacey, V M Fernández, M Rousset *Coord. Chem. Rev.* **249** 1596 (2005)

105. A L De Lacey, V M Fernández, M Rousset, R Cammack *Chem. Rev.* **107** 4304 (2007)
106. H Ogata, K Nishikawa, W Lubitz *Nature (London)* **520** 571 (2015)
107. S Canaguier, V Artero, M Fontecave *Dalton Trans.* 315 (2008)
108. C-H Lai, J H Reibenspies, M Y Darensbourg *Angew. Chem., Int. Ed. Engl.* **35** 2390 (1996)
109. P A Stenson, A Marin-Becerra, C Wilson, A J Blake, J McMaster, M Schröder *Chem. Commun.* 317 (2006)
110. F Osterloh, W Saak, D Haase, S Pohl *Chem. Commun.* 979 (1997)
111. W-F Liaw, C-Y Chiang, G-H Lee, S-M Peng, C-H Lai, M Y Darensbourg *Inorg. Chem.* **39** 480 (2000)
112. S C Davies, D J Evans, D L Hughes, S Longhurst, J R Sanders *Chem. Commun.* 1935 (1999)
113. M C Smith, J E Barclay, S P Cramer, S C Davies, W-W Gu, D L Hughes, S Longhurst, D J Evans *J. Chem. Soc., Dalton Trans.* 2641 (2002)
114. W Zhu, A C Marr, Q Wang, F Neese, D J E Spencer, A J Blake, P A Cooke, C Wilson, M Schöder *Proc. Natl. Acad. Sci. USA* **102** 18280 (2005)
115. M A Reynolds, T B Rauchfuss, S R Wilson *Organometallics* **22** 1619 (2003)
116. D Sellmann, F Geipel, F Lauderbach, F W Heinemann *Angew. Chem., Int. Ed.* **41** 632 (2002)
117. J A W Verhagen, D D Ellis, M Lutz, A L Spek, E Bouwman *J. Chem. Soc., Dalton Trans.* 1275 (2002)
118. J A W Verhagen, M Lutz, A L Spek, E Bouwman *Eur. J. Inorg. Chem.* 3968 (2003)
119. Z Li, Y Ohki, K Tatsumi *J. Am. Chem. Soc.* **127** 8950 (2005)
120. S Ogo, K Ichikawa, T Kishima, T Matsumoto, H Nakai, K Kusaka, T Ohhara *Science* **339** 682 (2013)
121. A Perra, E S Davies, J R Hyde, Q Wang, J McMaster, M Schröder *Chem. Commun.* 1103 (2006)
122. D Sellmann, F Lauderbach, F Geipel, F W Heinemann, M Moll *Angew. Chem. Int. Ed.* **43** 3141 (2004)
123. F Lauderbach, R Prakash, A W Götz, M Munoz, F W Heinemann, U Nickel, B A Hess, D Sellmann *Eur. J. Inorg. Chem.* 3385 (2007)
124. L-C Song, X-J Sun, G -J Jia, M-M Wang, H-B Song *J. Organomet. Chem.* **761** 10 (2014)
125. B C Manor, T B Rauchfuss *J. Am. Chem. Soc.* **135** 11895 (2013)
126. B C Manor, M R Ringenberg, T B Rauchfuss *Inorg. Chem.* **53** 7241 (2014)
127. R M Bullock, M L Helm *Acc. Chem. Res.* **48** 2017 (2015)
128. T Liu, Q Liao, M O'Hagan, E B Hulley, D L DuBois, R M Bullock *Organometallics* **34** 2747 (2015)
129. T Liu, S Chen, M J O'Hagan, M R DuBois, R M Bullock, D L DuBois *J. Am. Chem. Soc.* **134** 6257 (2012)
130. J M Parmon, S Raugei, T Liu, E B Hulley, C J Weiss, R M Bullock, M L Helm *ACS Cat.* **4** 1246 (2014)
131. V V Khrizanforova, E I Musina, M N Khrizanforov, T P Gerasimova, S A Katsyuba, Yu S Spiridonova, D R Islamov, O N Kataeva, A A Karasik, O G Sinyashin, Yu H Budnikova *J. Organomet. Chem.* **789** 14 (2015)
132. E I Musina, V V Khrizanforova, I D Strelnik, M I Valitov, Y S Spiridonova, D B Krivolapov, I A Litvinov, M K Kadirov, P Lönnecke, E Hey-Hawkins, Yu H Budnikova, A A Karasik, O G Sinyashin *Chem. – Eur. J.* **20** 3169 (2014)
133. V V Khrizanforova, Yu G Budnikova, I D Strelnik, E I Musina, M I Valitov, M K Kadirov, A A Karasik, O G Sinyashin *Russ. Chem. Bull., Int. Ed.* **62** 1003 (2013)
134. Yu H Budnikova, V V Khrizanforova, R M Galimullina, A A Karasik, E I Musina, A R Burilov, O G Sinyashin *Phosphorus, Sulphur, Silicon Relat. Elem.* **188** 84 (2013)
135. D H Pool, M P Stewart, M O'Hagan, W J Shaw, J A S Roberts, R M Bullock, D L DuBois *Proc. Natl. Acad. Sci. USA* **109** 15634 (2012)
136. U J Kilgore, J A S Roberts, D H Pool, A M Appel, M P Stewart, M Rakowski DuBois, W G Dougherty, W S Kassel, R M Bullock, D L DuBois *J. Am. Chem. Soc.* **133** 5861 (2011)
137. J Hou, M Fang, A J P Cardenas, W J Shaw, M L Helm, R M Bullock, J A S Roberts, M O'Hagan *Energy Environ. Sci.* **7** 4013 (2014)
138. U J Kilgore, M P Stewart, M L Helm, W G Dougherty, W S Kassel, M Rakowski DuBois, D L DuBois, R M Bullock *Inorg. Chem.* **50** 10908 (2011)
139. J Y Yang, S Chen, W G Dougherty, W S Kassel, R M Bullock, D L DuBois, S Raugei, R Rousseau, M Dupuis, M Rakowski DuBois *Chem. Commun.* **46** 8618 (2010)
140. A D Wilson, R H Newell, M J McNevin, J T Muckerman, M Rakowski DuBois, D L DuBois *J. Am. Chem. Soc.* **128** 358 (2006)
141. J Y Yang, S E Smith, T Liu, W G Dougherty, W A Hoffert, W S Kassel, M Rakowski DuBois, D L DuBois, R M Bullock *J. Am. Chem. Soc.* **135** 9700 (2013)
142. A Dutta, J A S Roberts, W J Shaw *Angew. Chem., Int. Ed.* **53** 6487 (2014)
143. A Dutta, S Lense, J Hou, M H Engelhard, J A S Roberts, W J Shaw *J. Am. Chem. Soc.* **135** 18490 (2013)
144. S E Smith, J Y Yang, D L DuBois, R M Bullock *Angew. Chem., Int. Ed.* **51** 3152 (2012)
145. V Artero, J-M Savéant *Energy Environ. Sci.* **7** 3808 (2014)
146. G A N Felton, A K Vanucci, N Okumura, L T Lockett, D H Evans, R S Glass, D L Lichtenberger *Organometallics* **27** 4671 (2008)
147. C C L McCrory, C Uyeda, J C Peters *J. Am. Chem. Soc.* **134** 3164 (2012)
148. C Costentin, M Robert, J-M Savéant *Chem. Soc. Rev.* **42** 2423 (2013)
149. C Costentin, J-M Savéant *ChemElectroChem* **1** 1226 (2014)
150. C Costentin, S Drouet, M Robert, J-M Savéant *J. Am. Chem. Soc.* **134** 11235 (2012)
151. F Quentel, F Gloaguen *Electrochim. Acta* **110** 641 (2013)
152. P Surawatanawong, J W Tye, M Y Darensbourg, M B Hall *Dalton Trans.* **39** 3093 (2010)
153. E S Donovan, G S Nichol, G A N Felton *J. Organomet. Chem.* **726** 9 (2013)
154. K Weber, T Weyhermüller, E Bill, Ö F Erdem, W Lubitz *Inorg. Chem.* **54** 6928 (2015)
155. K P Butin, E K Beloglazkina, N V Zyk *Russ. Chem. Rev.* **74** 531 (2005)
156. Yu H Budnikova *Russ. Chem. Rev.* **71** 111 (2002)
157. V A Milyukov, Yu H Budnikova, O G Sinyashin *Russ. Chem. Rev.* **74** 781 (2005)
158. D Yu Mikhailov, Yu H Budnikova *Russ. Chem. Rev.* **82** 835 (2013)
159. Yu H Budnikova, O G Sinyashin *Russ. Chem. Rev.* **84** 917 (2015)
160. M N Elinson, E O Dorofeeva, A N Vereshchagin, G I Nikishin *Russ. Chem. Rev.* **84** 485 (2015)
161. A V Shchepochkin, O N Chupakhin, V N Charushin, V A Petrosyan *Russ. Chem. Rev.* **82** 747 (2013)
162. C Léger, P Bertrand *Chem. Rev.* **108** 2379 (2008)
163. C Costentin *Chem. Rev.* **108** 2145 (2008)
164. A Houmam *Chem. Rev.* **108** 2180 (2008)
165. V V Kondratiev, V V Malev, S N Eliseeva *Russ. Chem. Rev.* **85** 14 (2016)
166. O A Petrii *Russ. Chem. Rev.* **84** 159 (2015)